Electronic Supplementary Material (ESI) for Catalysis Science & Technology.

Rh nanoparticles from thiolate dimers: selective and reusable hydrogenation catalysts in ionic liquids

A. Serrano-Maldonado,* S. S. Rozenel, , J. L. Jimenez-Santiago, I. Guerrero-Ríos* and E. Martin†

Electronic Supplementary Information

Table of contents:

Figure S1. ^{1}H NMR of $[Rh(\mu\text{-}SC_{12}H_{25})(COD)]_2$ (I)

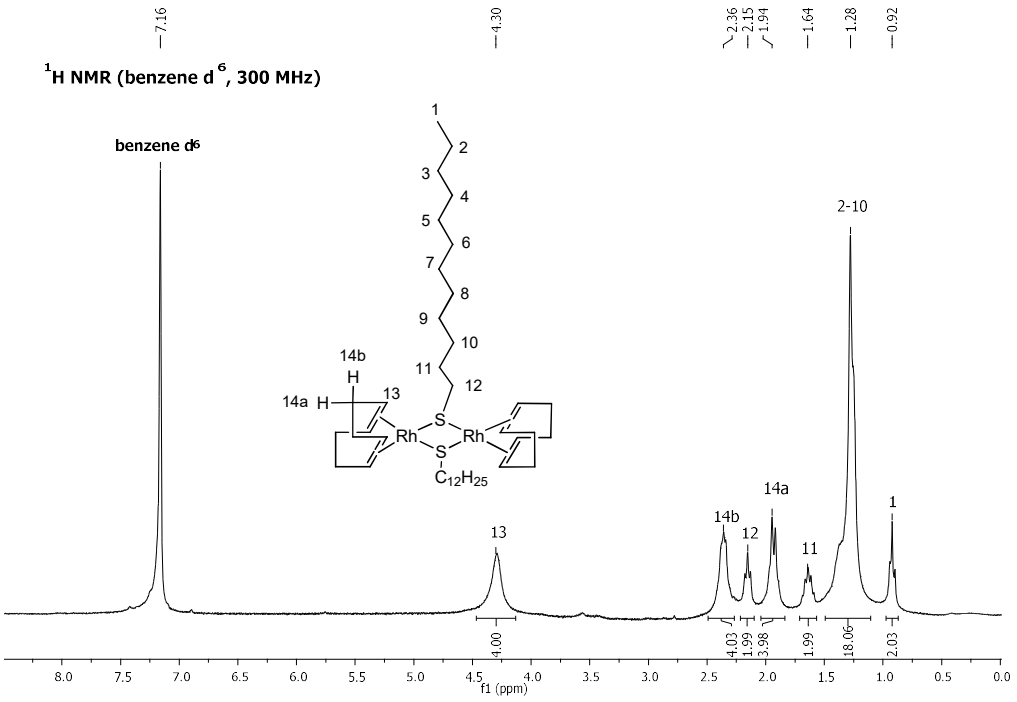

Figure S2. {^{1}H} COSY NMR of $[Rh(\mu\text{-}SC_{12}H_{25})(COD)]_2$ (I)

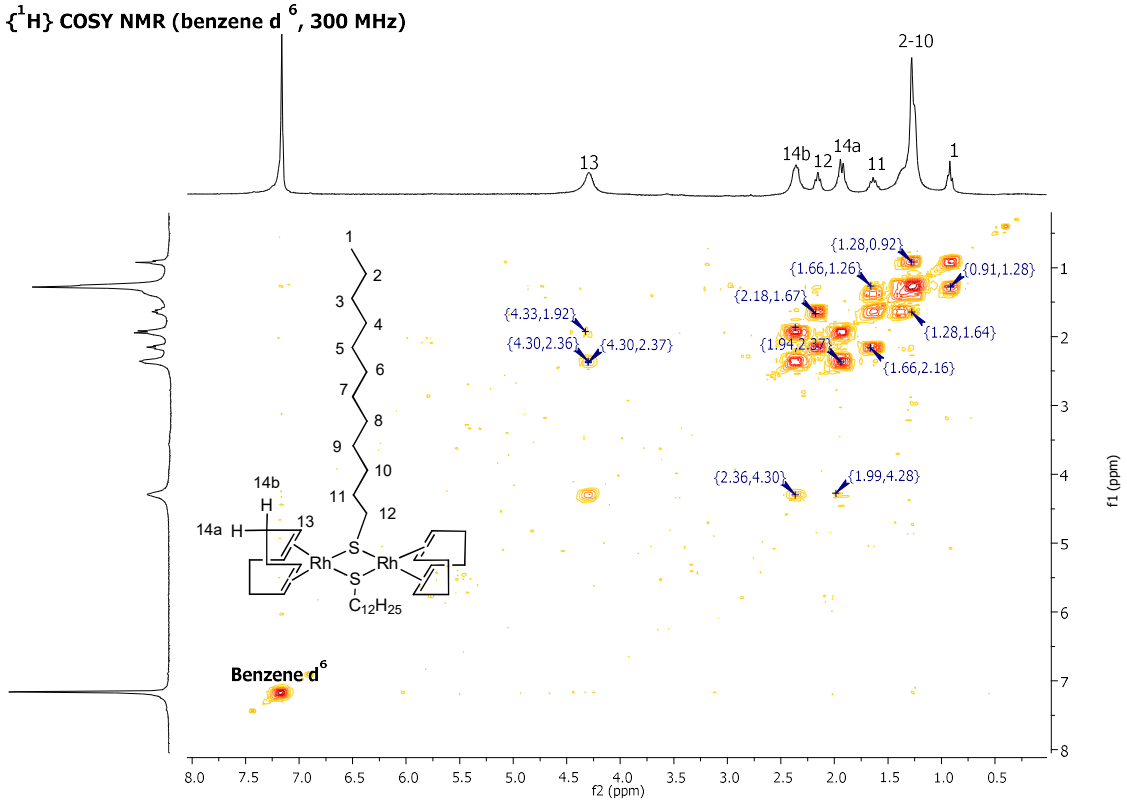

Figure S3. ^{13}C NMR of [Rh(μ-SC$_{12}$H$_{25}$)(COD)]$_2$ (I)

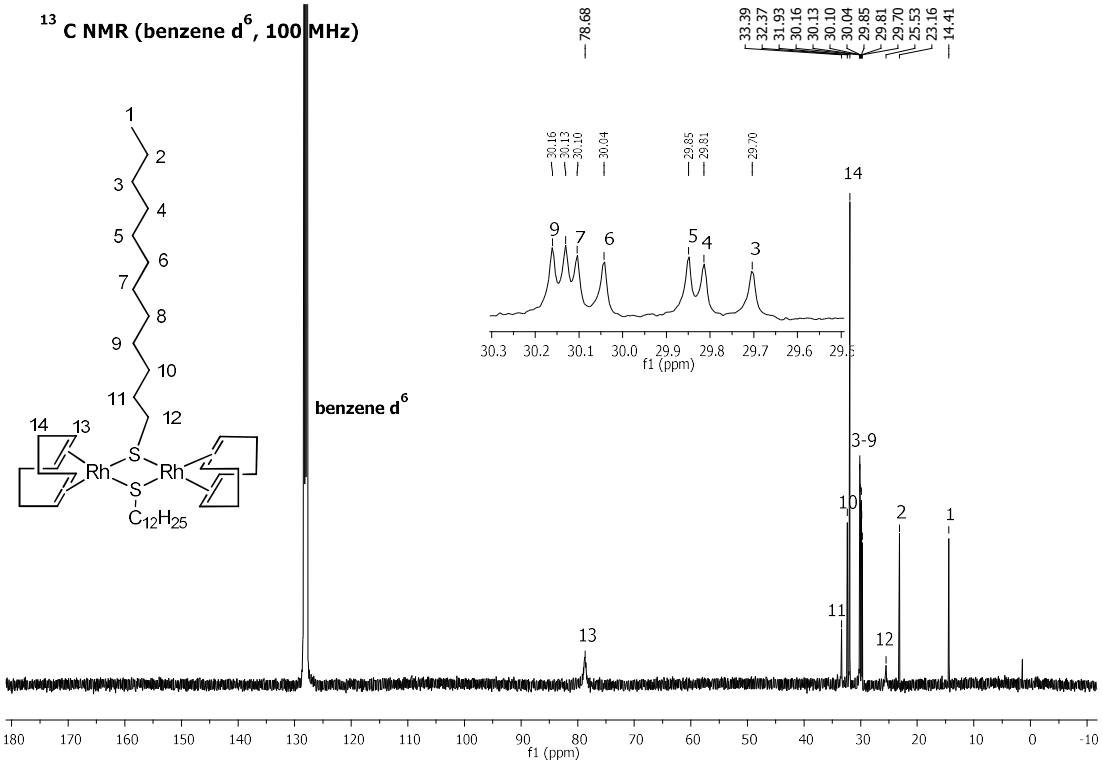

Figure S4. HSQC NMR of [Rh(μ-SC$_{12}$H$_{25}$)(COD)]$_2$ (I)

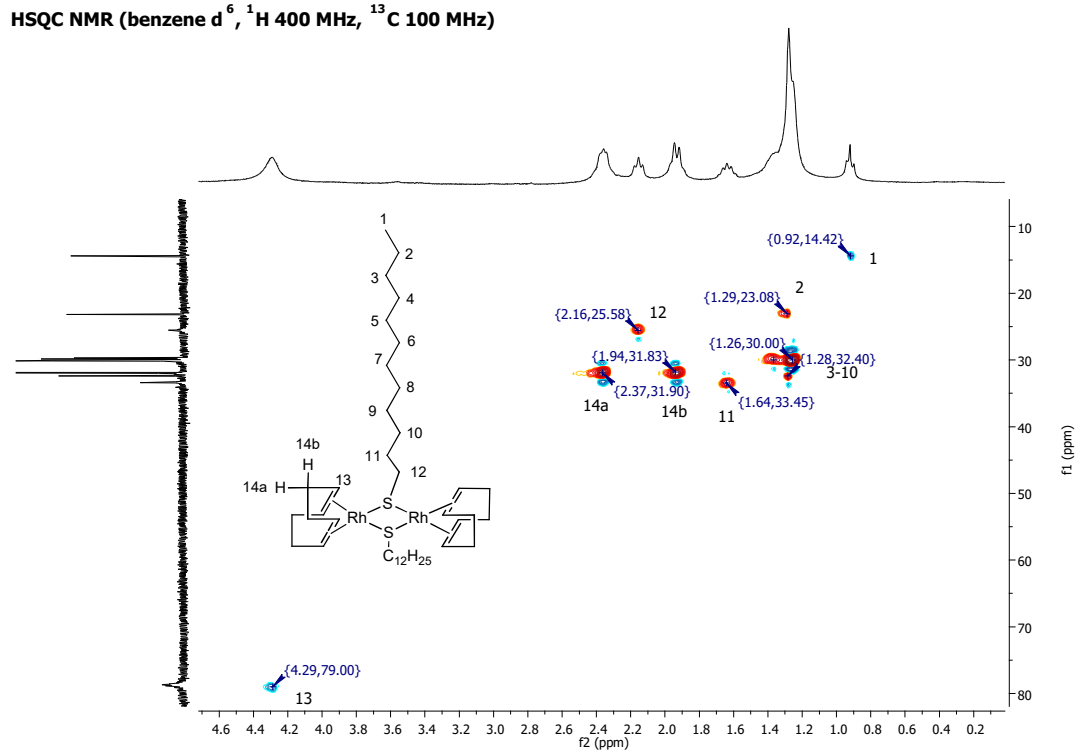

Figure S5. HMBC NMR of [Rh(μ-$SC_{12}H_{25}$)(COD)]$_2$ (I)

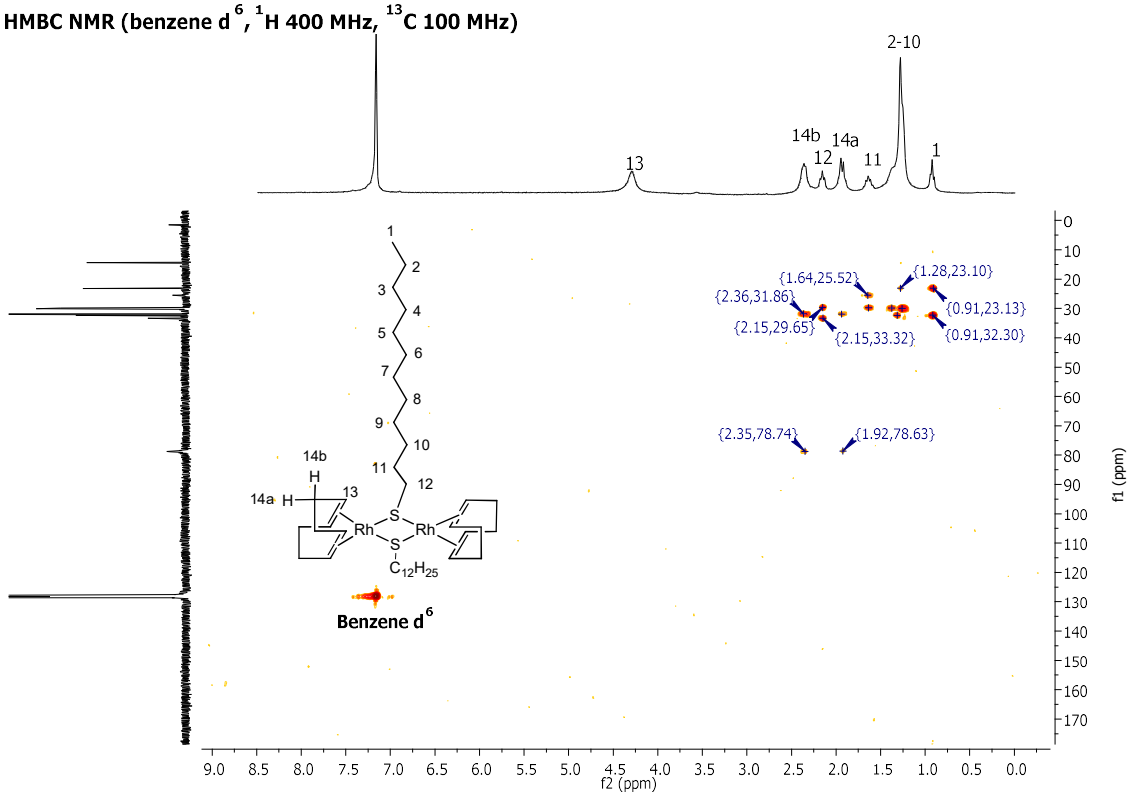

Figure S6. FTIR (KBr) of [Rh(μ-$SC_{12}H_{25}$)(COD)]$_2$ (I)

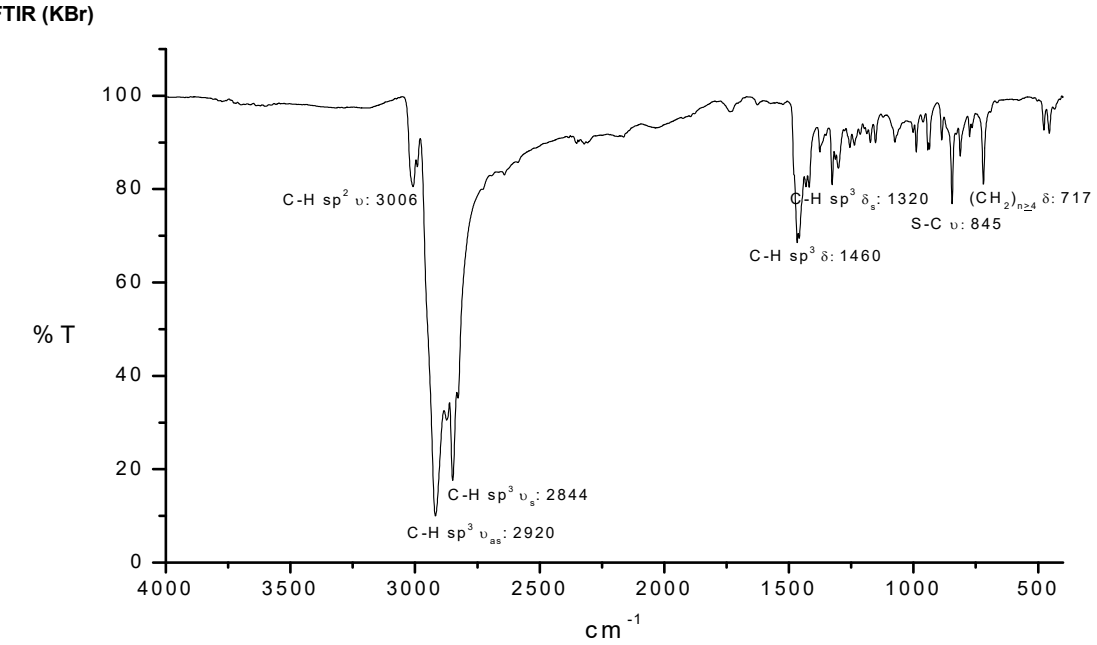

Figure S7. MS-FAB$^+$ of [Rh(μ-$SC_{12}H_{25}$)(COD)]$_2$ (I)

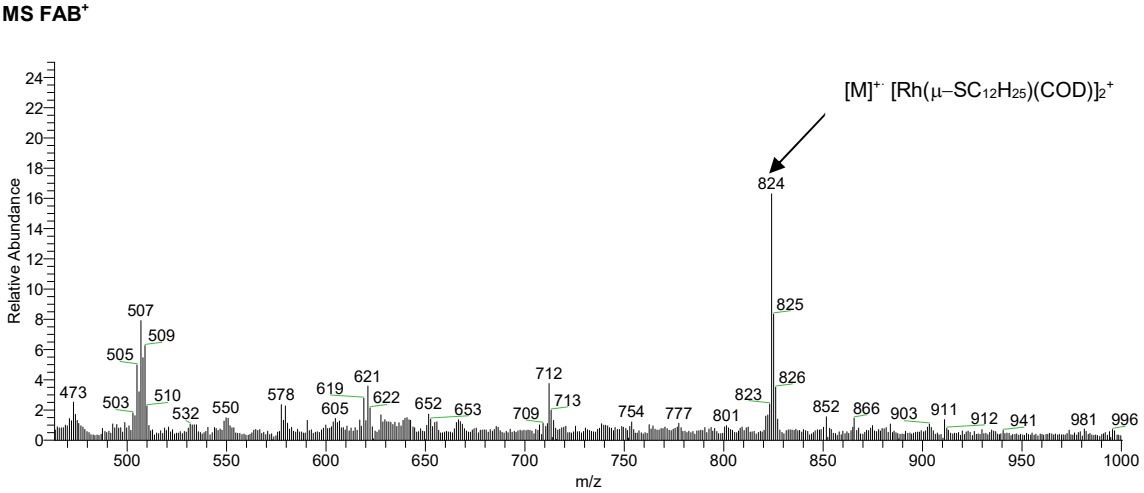

Figure S8. ^{1}H NMR of [Rh(μ-SC_6H_{11})(COD)]$_2$ (II)

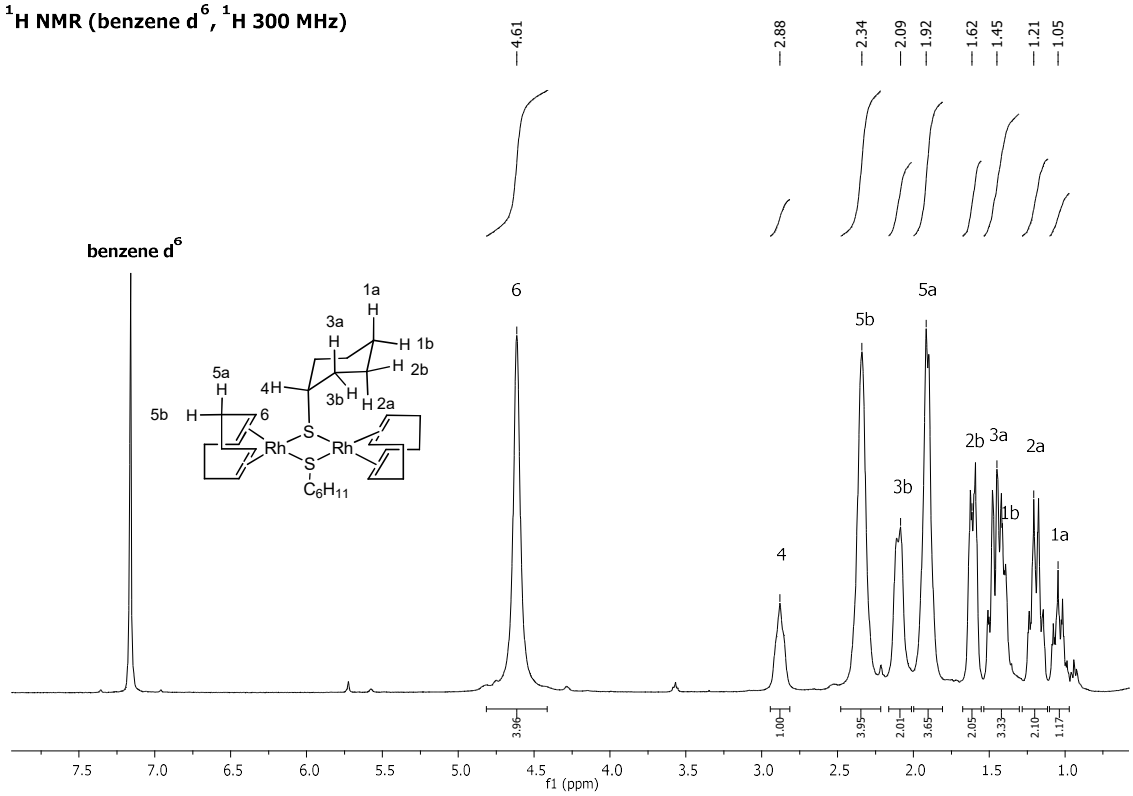

Figure S9. ^{1}H NMR of $[Rh(\mu\text{-}SC_6H_{11})(COD)]_2$ (II)

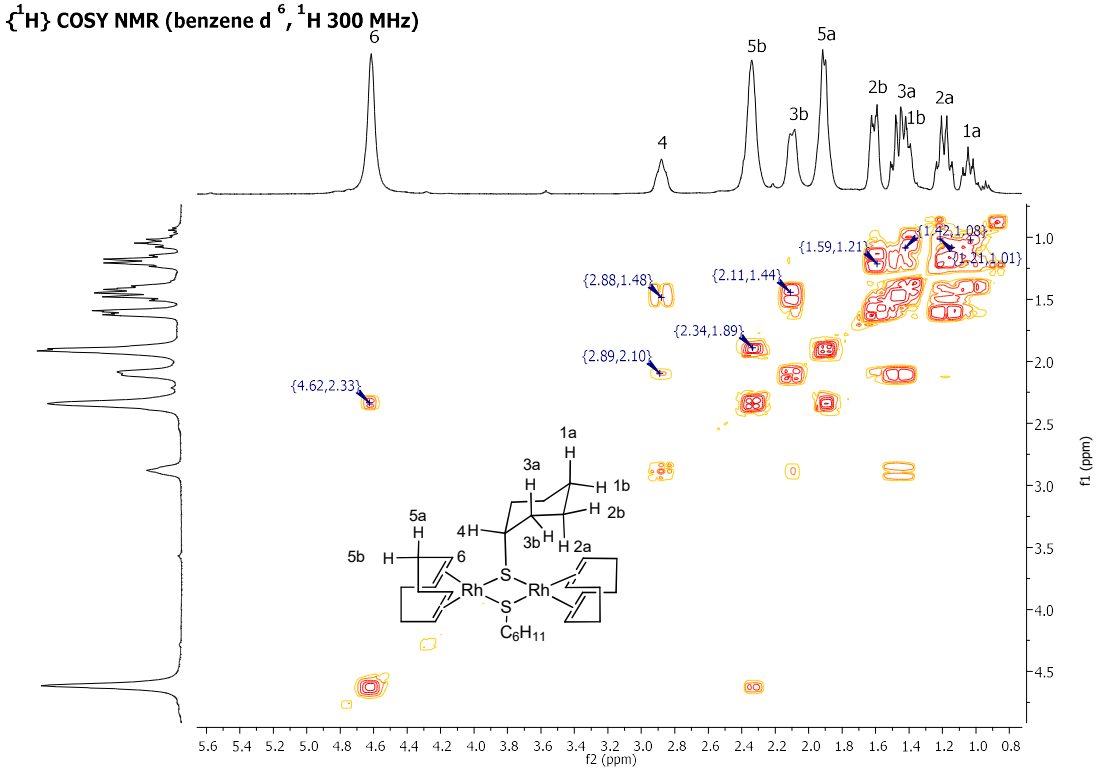

Figure S10. ^{13}C NMR of $[Rh(\mu\text{-}SC_6H_{11})(COD)]_2$ (II)

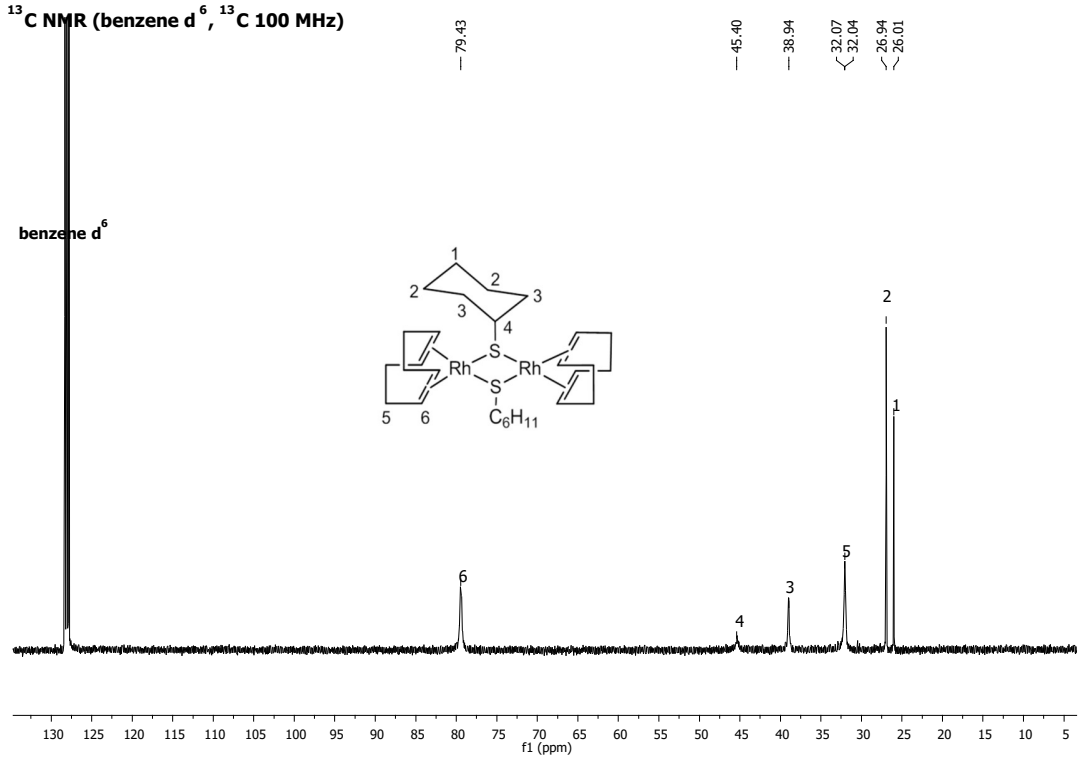

Figure S11. HSQC NMR of [Rh(μ-SC_6H_{11})(COD)]$_2$ (II)

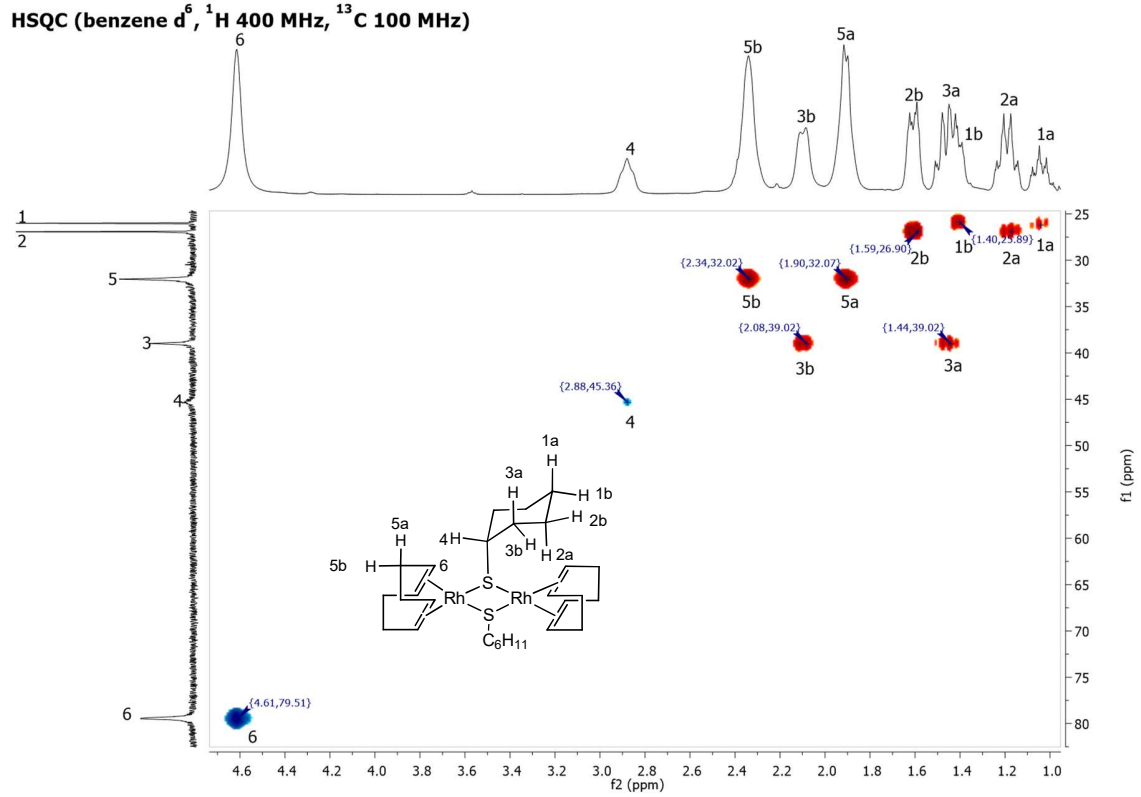

Figure S12. FTIR (KBr) of [Rh(μ-SC_6H_{11})(COD)]$_2$ (II)

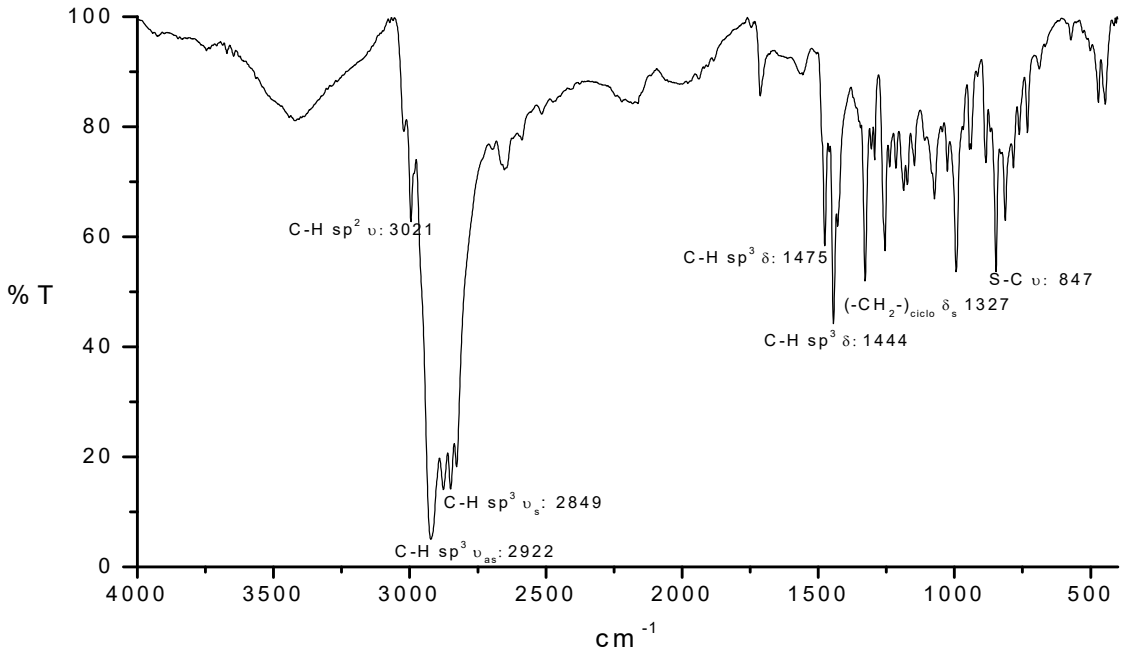

Figure S13. MS-FAB$^+$ of [Rh(μ-SC_6H_{11})(COD)]$_2$ (II)

MS FAB$^+$

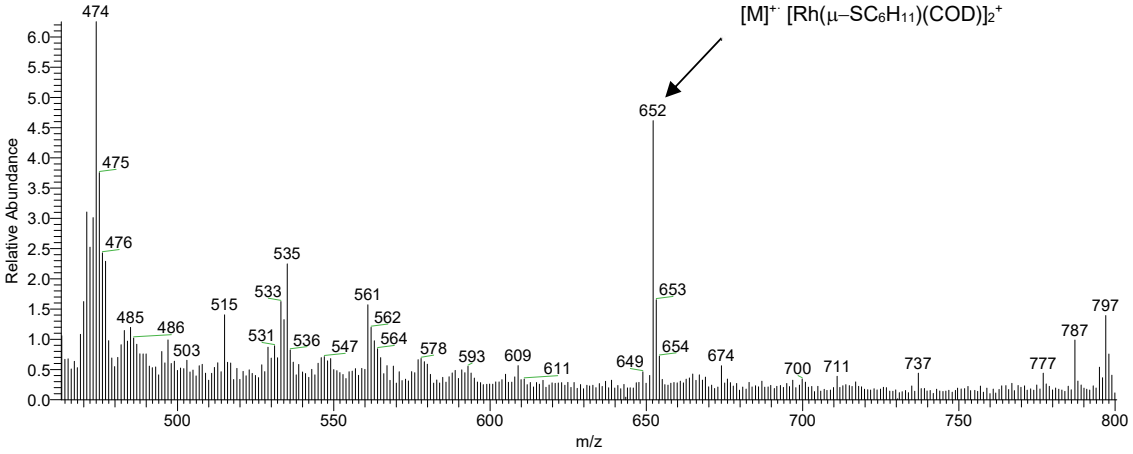

Figure S14. MS HR-ESI$^+$

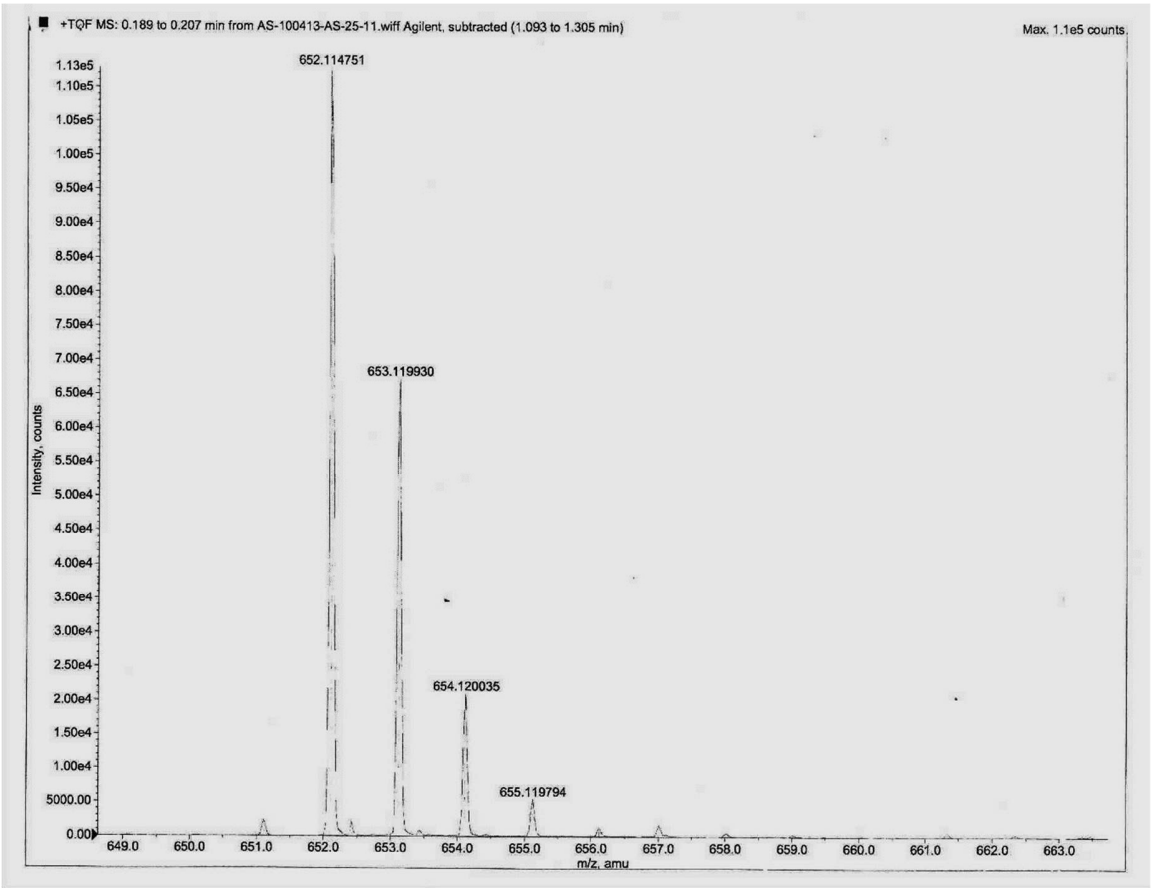

Figure S15. TEM images, size distribution and EDX of RhNPs-A

Mean diameter D = 2.66±0.22 nm

TEM images

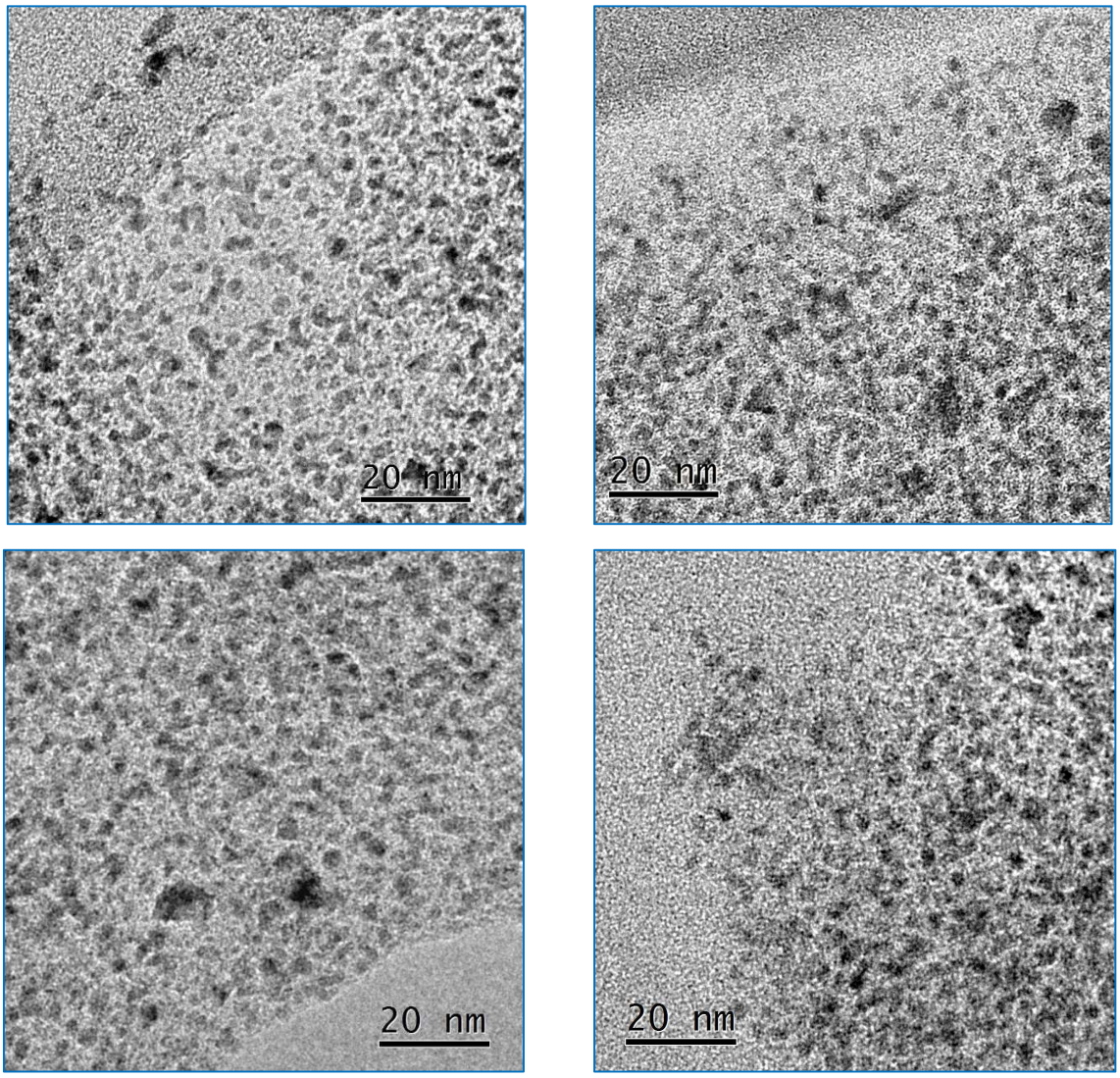

Size distribution and EDS

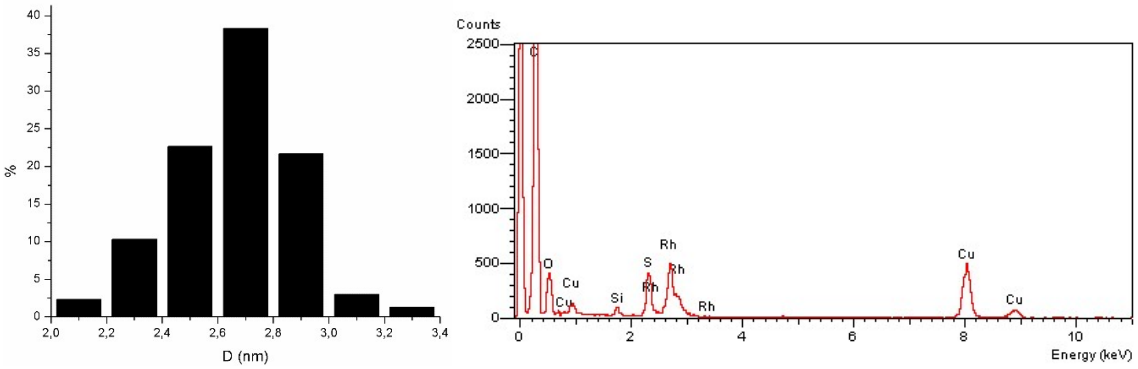

Figure S16. TEM images, size distribution and EDX of RhNPs-B

Mean diameter D = 2.81±0.26 nm

TEM Images

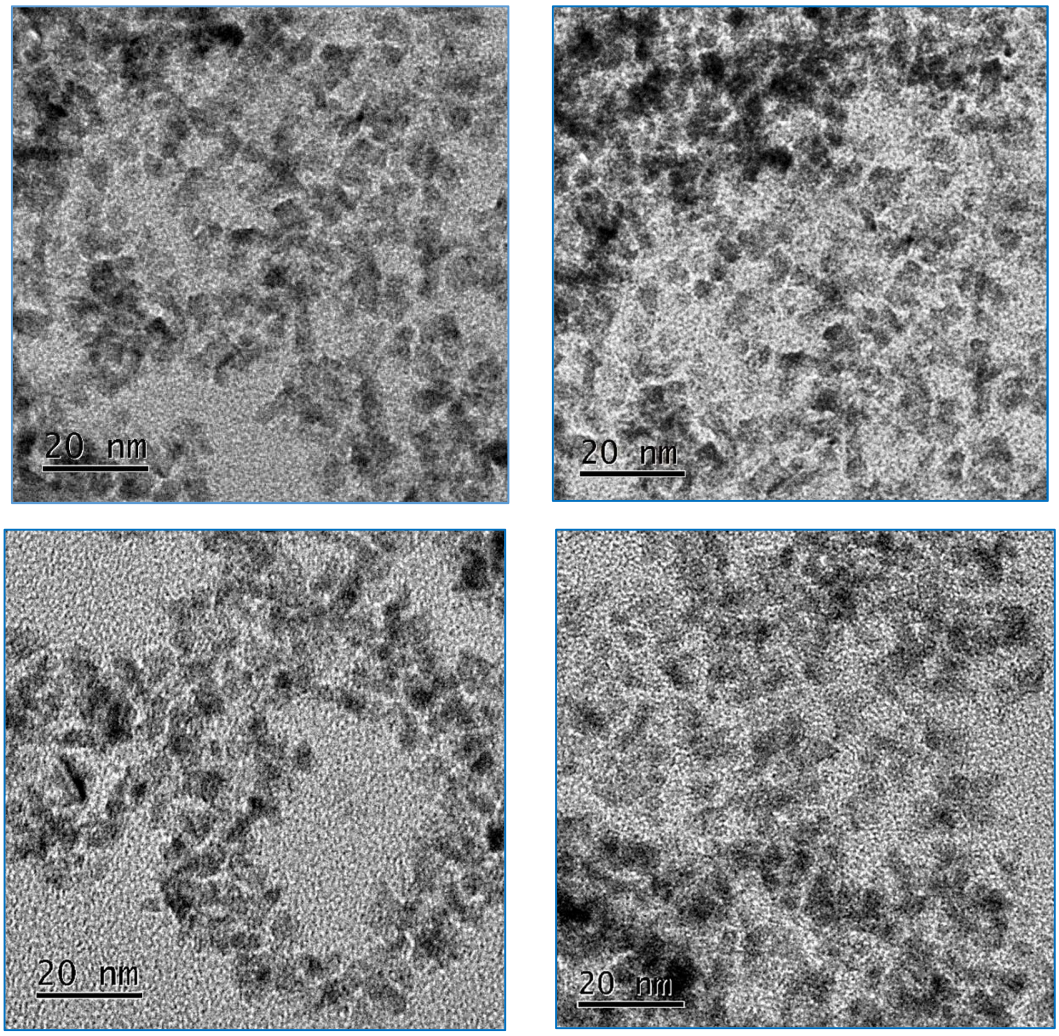

Size distribution and EDS

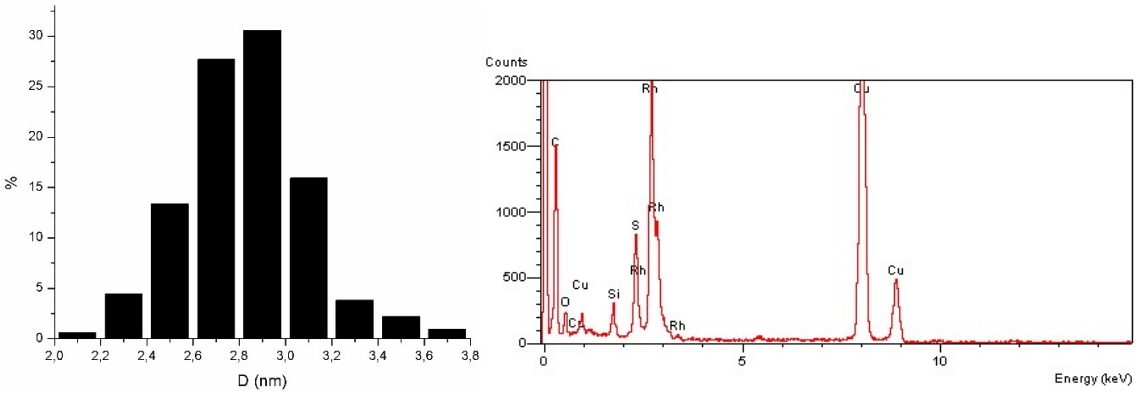

X

Figure S17. TEM images, size distribution and EDX of RhNPs-A/THF

Mean diameter D = 2.82±0.28 nm

TEM images

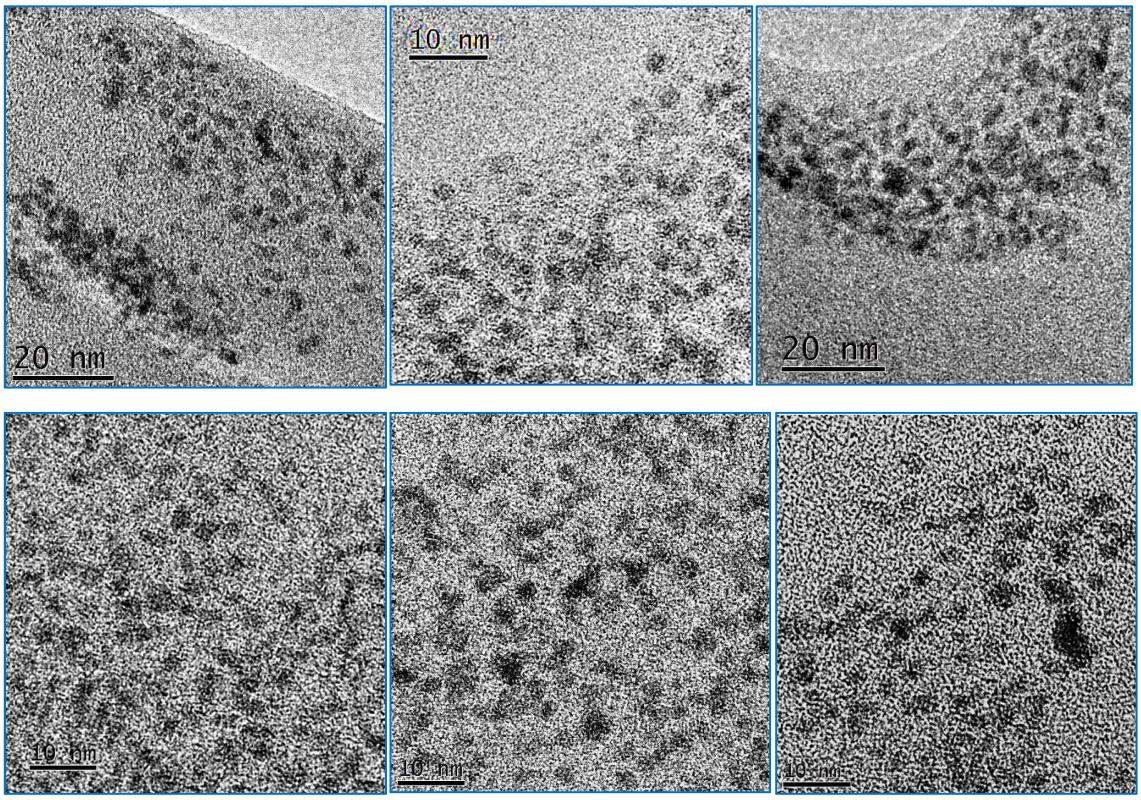

Size distribution and EDS

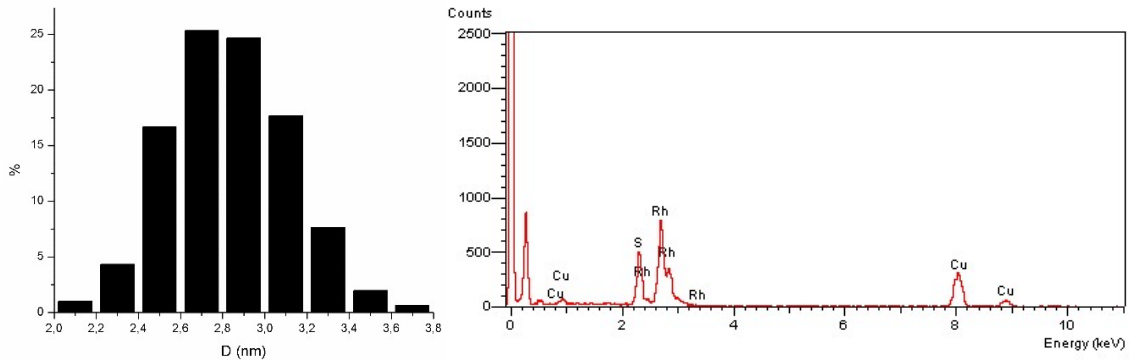

Figure S18. TEM images, size distribution and EDX of RhNPs-B/THF

Mean diameter D = 2.28±0.30 nm

TEM images

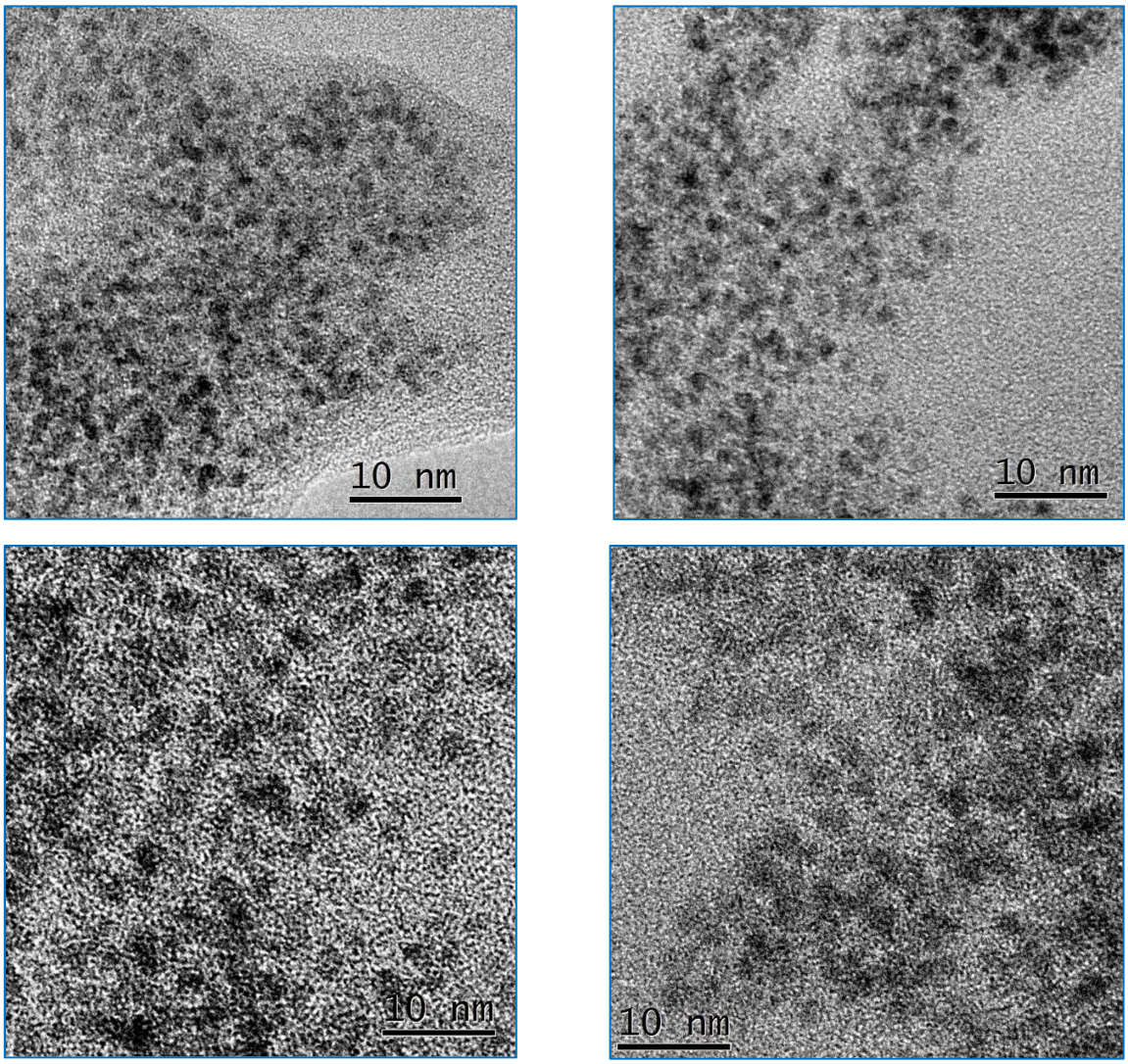

Size distribution and EDS

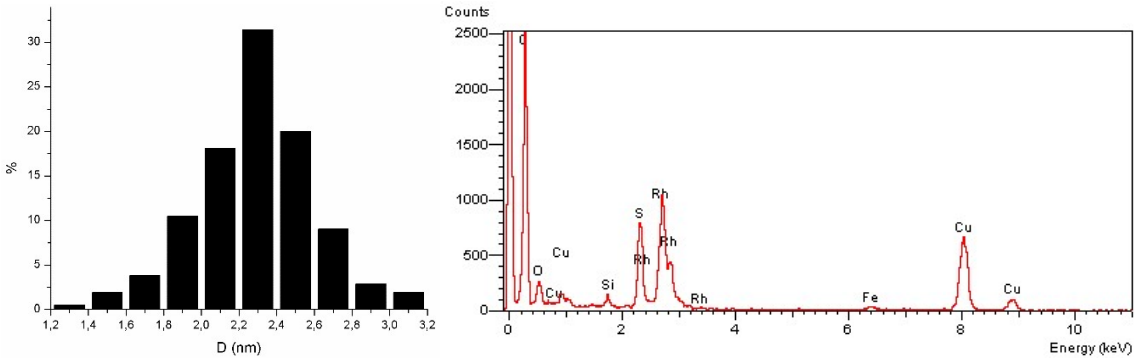

Figure S19. TEM images of RhNPs-B after 10 catalytic runs in styrene hydrogenation

Mean diameter D = 2.93±0.28 nm

TEM Images

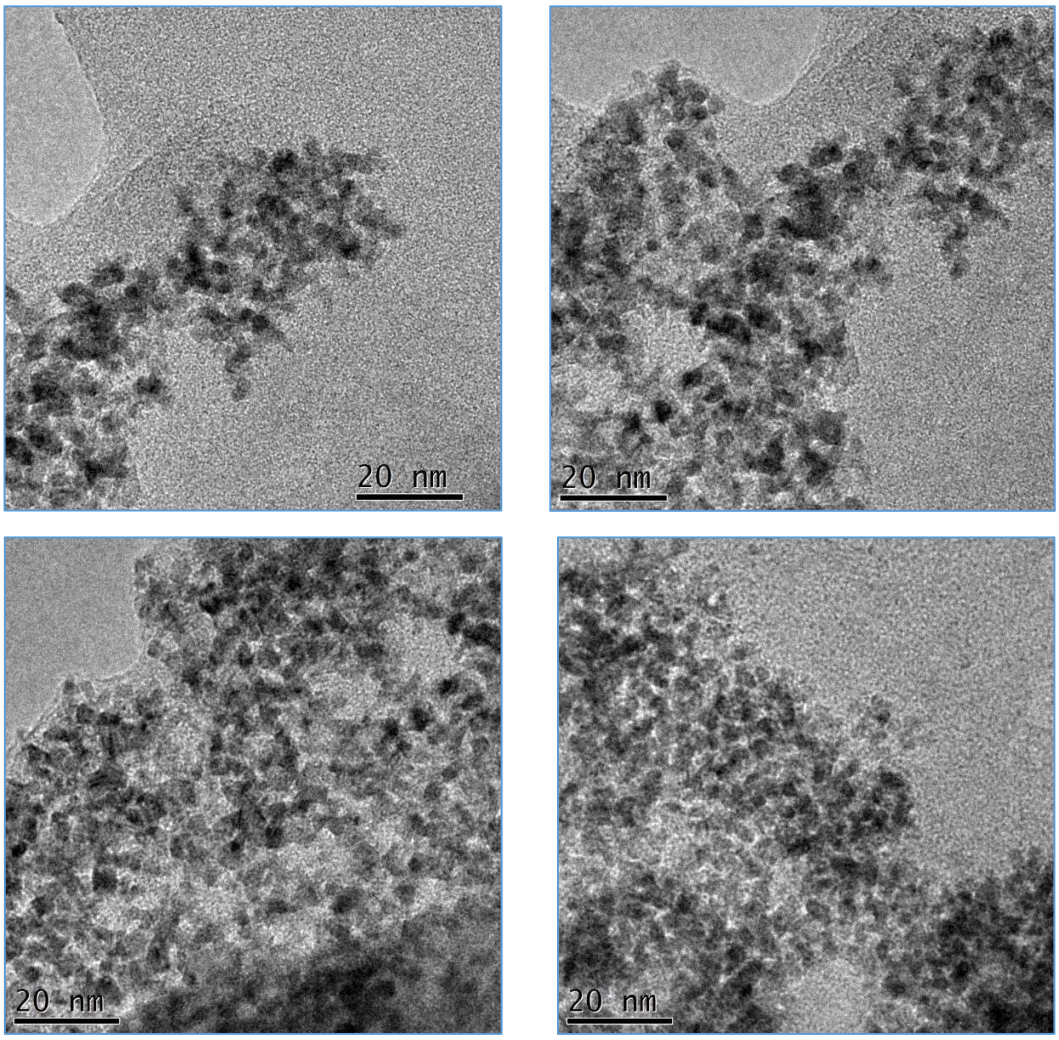

Size disribution and EDS

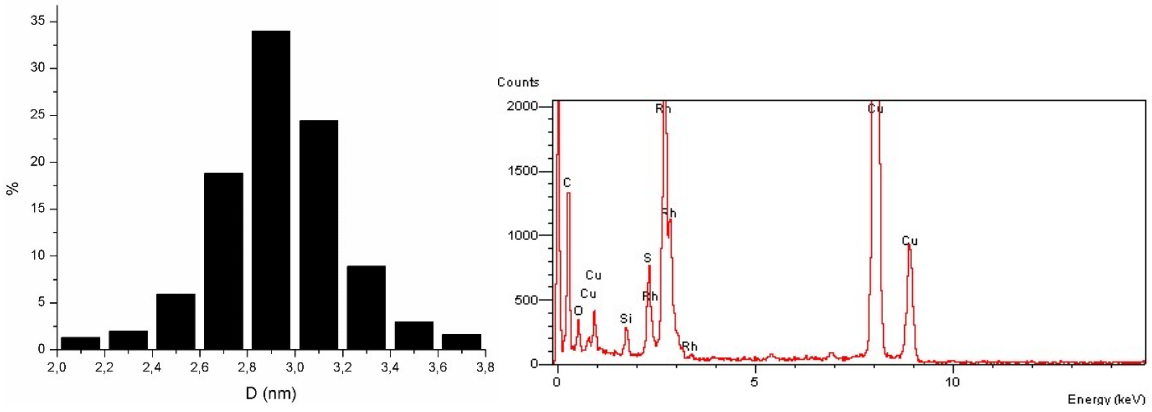

Figure S20. TEM images of RhNPs-B after 8 catalytic runs in *one-pot* multi-step synthesis of *N*-benzylaniline

TEM Images

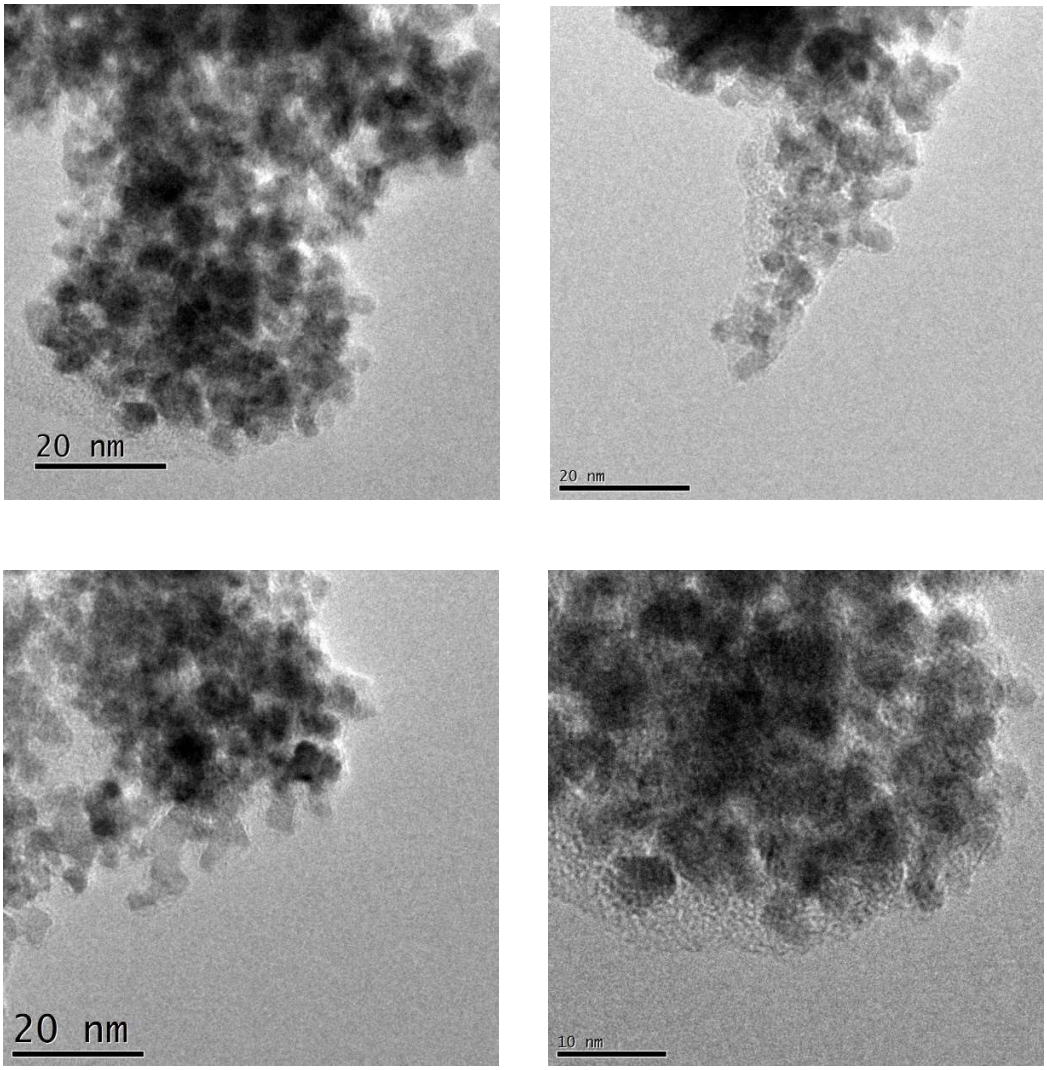

Figure S21. RhNPs-B XPS survey spectrum

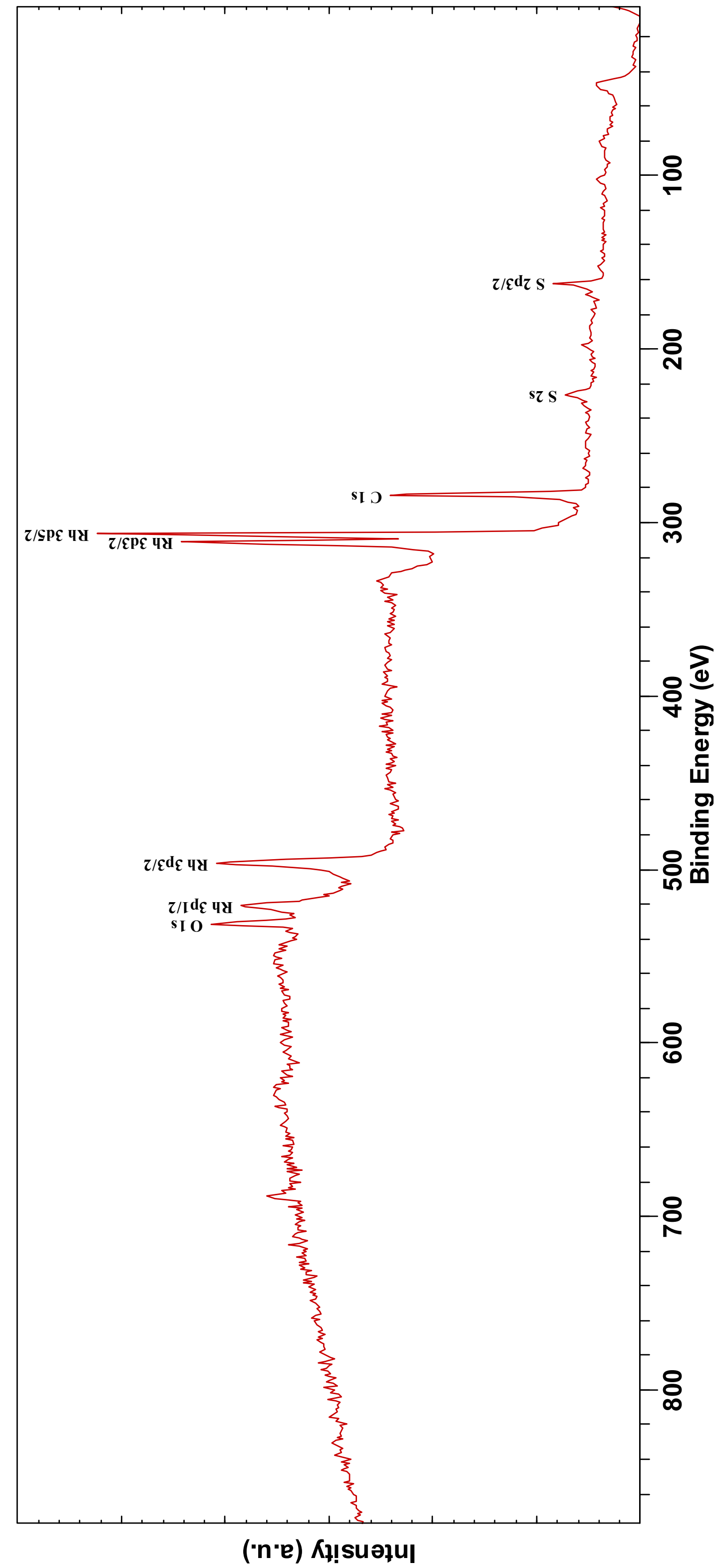

Figure S22. RhNPs-B high-resolution XPS spectra of Rh 3d and S 2s regions

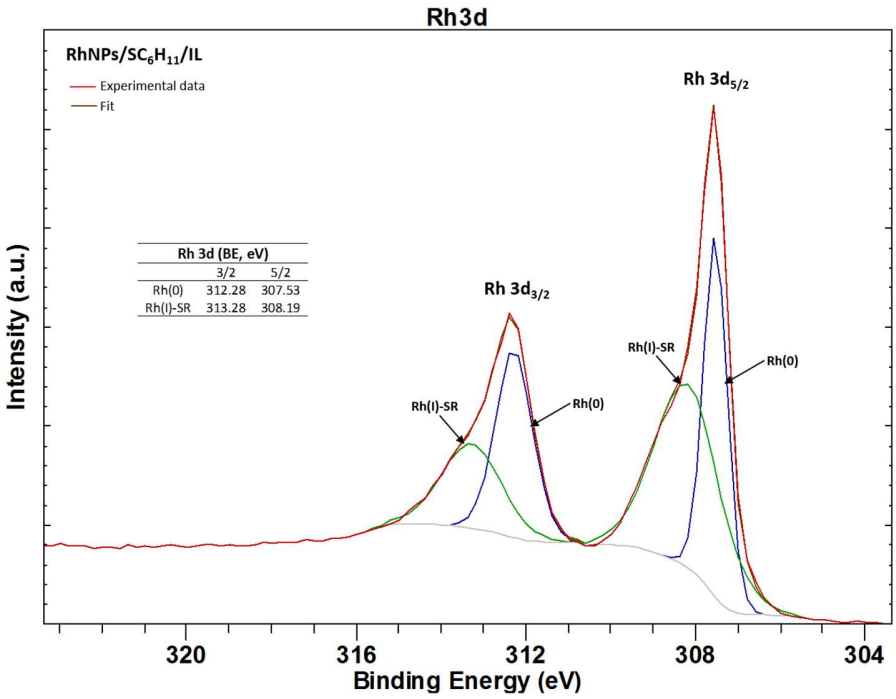

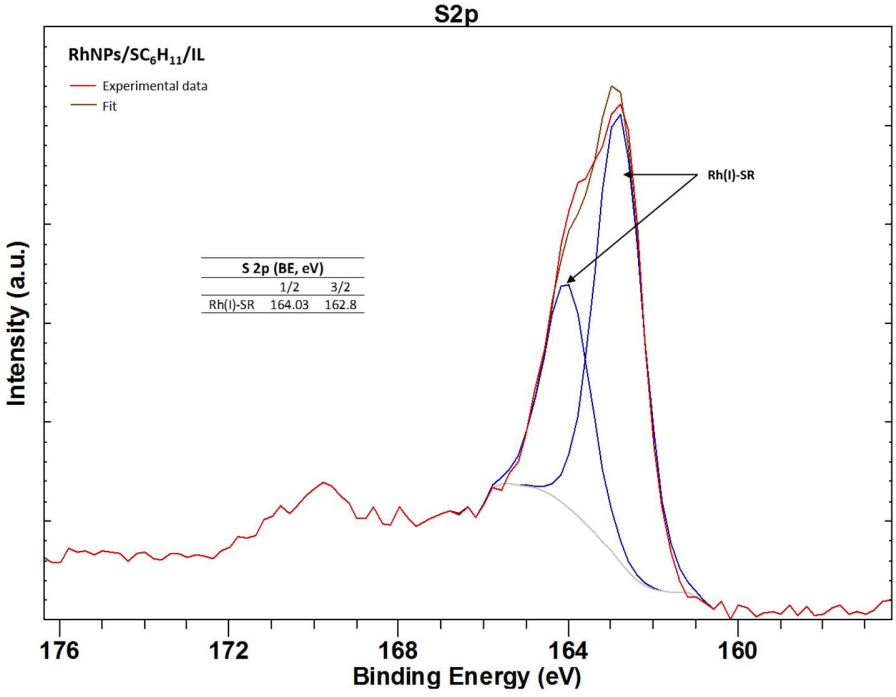

Figure S23. RhNPs-B/THF XPS survey spectrum

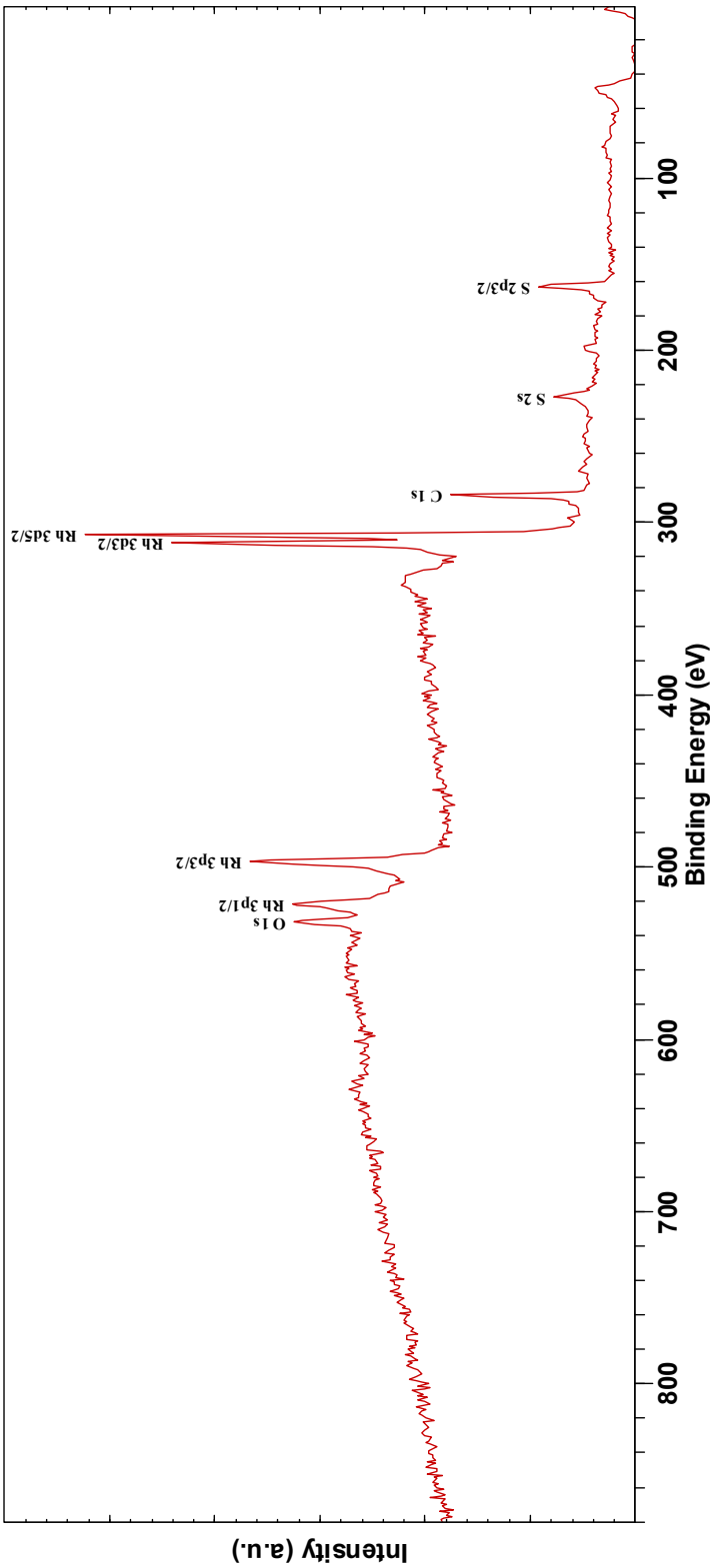

Figure S24. RhNPs-B/THF high-resolution XPS spectra of Rh 3d and S 2s regions

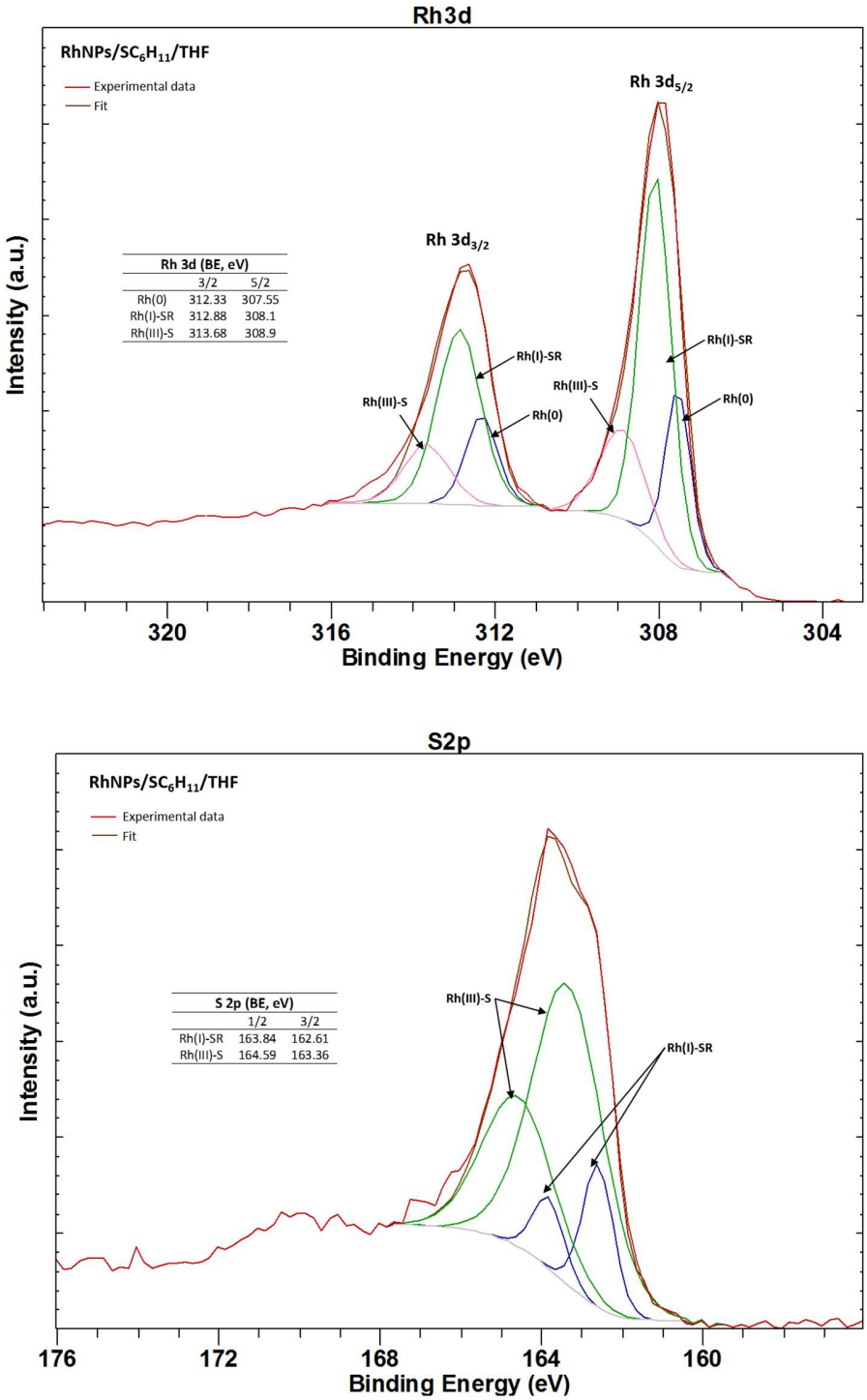

Figure S25. $[Rh(\mu\text{-}SC_6H_{11})(COD)]_2$ (II) high-resolution XPS spectra of Rh 3d and S 2s regions

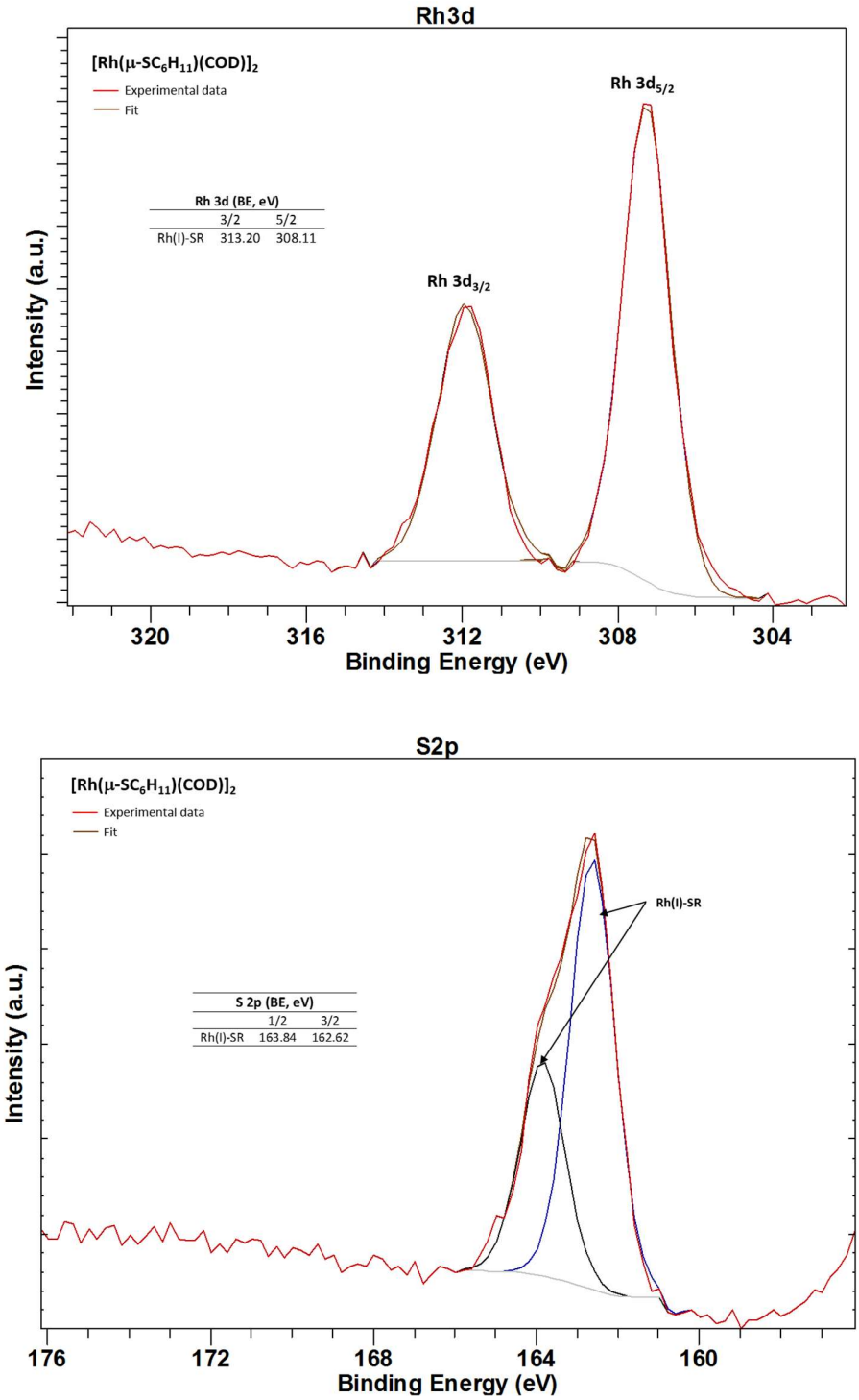

Figure S26. Effect of the pressure on the hydrogenation of styrene (1) using RhNPs as catalyst.

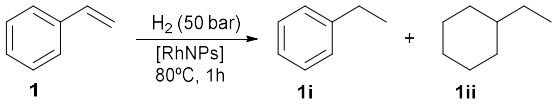

	Conversion (%)	Selectivity (%)	
RhNPs-A =	>99	99	-
RhNPs-B =	>99	99	-
RhNPs-C =	>99	92	8

General conditions: 1 mmol of styrene (**2**) and 1 mL of the catalytic solution of **RhNPs** (10^{-2} mol L^{-1}, 0.01 mmol of total Rh), 80°C, 1 hour.

Figure S27. Effect of the pressure on the hydrogenation of styrene (1) using thiolate-RhNPs as catalyst.

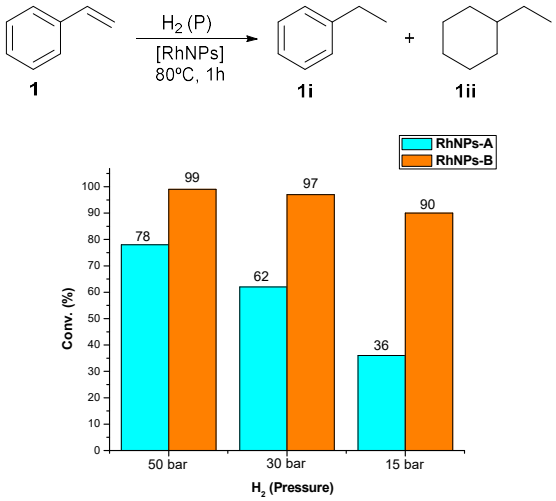

General conditions: 1 mmol of styrene (1) and 1 mL of the catalytic solution of **RhNPs** (10^{-2} mol L^{-1}, 0.01 mmol of total Rh), 80°C, 1 hour.

Table S1. Recycling experiments of styrene hydrogenation catalyzed by RhNPs-B

Catalytic run	1	2	3	4	5	6	7	8	9	10
Conv. (%)	90	93	91	90	92	88	92	93	89	87
Ethylbenzene (**1i**) sel. (%)	100	100	100	100	100	100	100	100	100	100

Recycling experiments of the catalytic system **RhNPs-B** in the hydrogenation of styrene (**1**). General conditions: 1 mmol of styrene (**1**) and 1 mL of the catalytic solution of **RhNPs-B** (10^{-2} mol L^{-1}, 0.01 mmol of total Rh), 80°C, *P* = 15 bar of H_2, 1 hour.

Figure S28. RhNPs-catalyzed acetophenone (2) hydrogenation

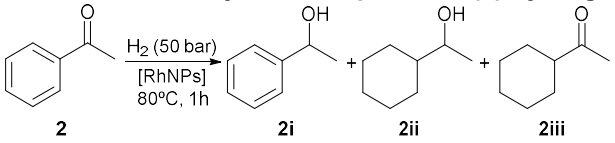

2 **2i** **2ii** **2iii**

Conversion (%)	Selectivity (%)		
RhNPs-A = 0	-	-	-
RhNPs-B = 0	-	-	-
RhNPs-C = 82	72	14	14

Figure S29. RhNPs-catalyzed benzaldehyde (3) hydrogenation

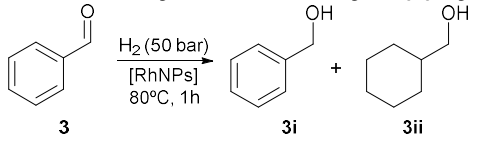

3 **3i** **3ii**

Conversion (%)	Selectivity (%)	
RhNPs-A = 0	-	-
RhNPs-B = 0	-	-
RhNPs-C = 23	90	10

Table S2. Selectivity comparison of RhNPs catalyzed hydrogenation of 4-phenyl-3-buten-2-one (4)

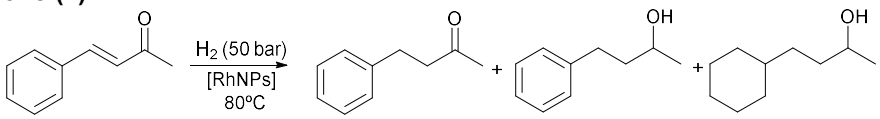

4 **4i** **4ii** **4iii**

Entry	Catalytic system	Time (h)	Conv. (%)[a]	Sel. **4i** (%)[a]	Sel. **4ii** (%)[a]	Sel. **4iii** (%)[a]
1	**RhNPs-A**	1	25	>99	-	-
2	**RhNPs-B**	1	78	>99	-	-
3	**RhNPs-C**	1	>99	79	11	10
4	**RhNPs-A**	2	55	>99	-	-
5	**RhNPs-B**	2	98	>99	-	-

Results from duplicated experiments. Reaction conditions: 1 mmol of 4-phenyl-3-buten-2-one and 1 mL of the catalytic solution of **RhNPs** (10^{-2} mol L^{-1}, 0.01 mmol of total Rh), H_2 (50 bar), 80°C. [a] Determined by GC using decane as internal standard.

Table S3. Recycling experiments of 4-phenyl-3-buten-2-one (4) hydrogenation catalyzed by RhNPs-B

Catalytic run	1	2	3	4	5	6	7	8	9	10
Conv. (%)	98	94	94	92	93	91	88	90	87	88
4-phenylbutanone (**4i**) sel. (%)	100	100	100	100	100	100	100	100	100	100

Recycling experiments of the catalytic system **RhNPs-B** in the hydrogenation of 4-phenyl-3-buten-2-one (**4**). General conditions: 1 mmol of 4-phenyl-3-buten-2-one (**4**) and 1 mL of the catalytic solution of **RhNPs-B** (10^{-2} mol L^{-1}, 0.01 mmol of total Rh), 80°C, P = 50 bar of H_2, 1 hour.

Figure S30. Evolution of conversion in the RhNPs-catalyzed hydrogenation of 4-nitroacetophenone (5)

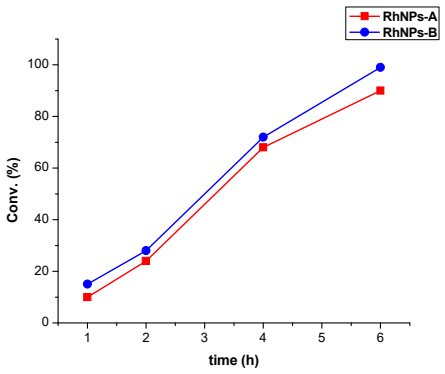

General conditions: 1 mmol of 4-nitroacetophenone and 1 mL of the catalytic solution of **RhNPs** (10^{-2} mol L^{-1}, 0.01 mmol of total Rh), 80°C, *P* = 50 bar of H_2.

Table S4. RhNPs-B catalyzed hydrogenation of *N*-benzylidenaniline (10)

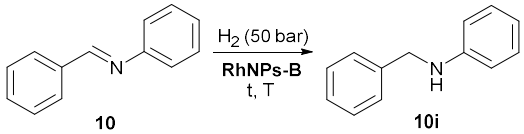

10 **10i**

Entry	Time (h)	Temp. (°C)	Conv. (Sel.) (%)[a]
1	1	80	5 (>99)
2	2	80	21 (>99)
3	2	100	27 (>99)
4	8	100	97 (>99)

Results from duplicated experiments. Reaction conditions: 1 mmol of *N*-benzylidenaniline and 1 mL of the catalytic solution of **RhNPs-B** (10^{-2} mol L^{-1}, 0.01 mmol of total Rh), H_2 (50 bar), 80°C. [a] Determined by GC using decane as internal standard.

Table S5 RhNPs-B catalyzed one-pot two-step synthesis of *N*-benzylaniline

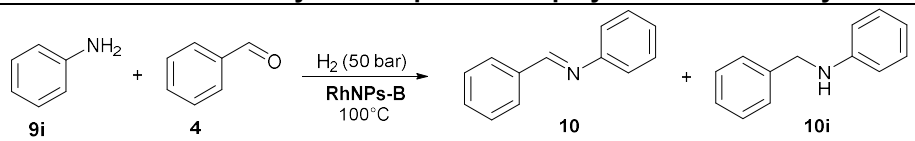

9i **4** **10** **10i**

Entry	Time (h)	Conv. (%)[a]	Selectivity **10/10i** (%)[a]
1	4	>99	40/60
2	8	>99	11/89
3	18	>99	3/97

Results from duplicated experiments. Reaction conditions: 1 mmol of aniline (**9i**), 1 mmol of benzaldehyde (**4**) and 1 mL of the catalytic solution of **RhNPs-B** (10^{-2} mol L^{-1}, 0.01 mmol of total Rh), H_2 (50 bar), 100°C. [a] Determined by GC using decane as internal standard.

Figure S31. ^{1}H NMR monitoring of RhNPs-A catalyzed hydrogenation of 4-nitroacetophenone (5)

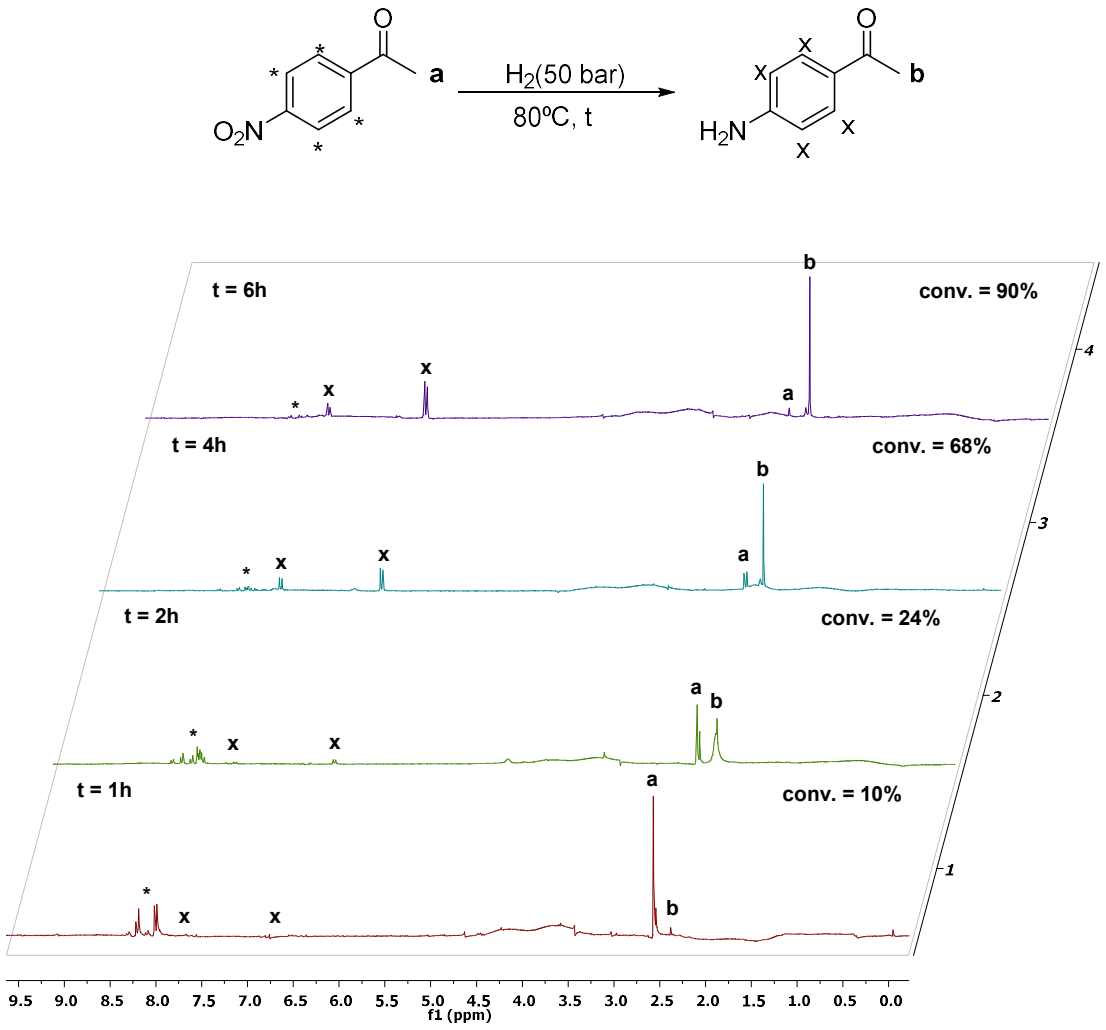

Figure S32. ^{1}H NMR monitoring of RhNPs-B catalyzed hydrogenation of 4-nitroacetophenone (5)

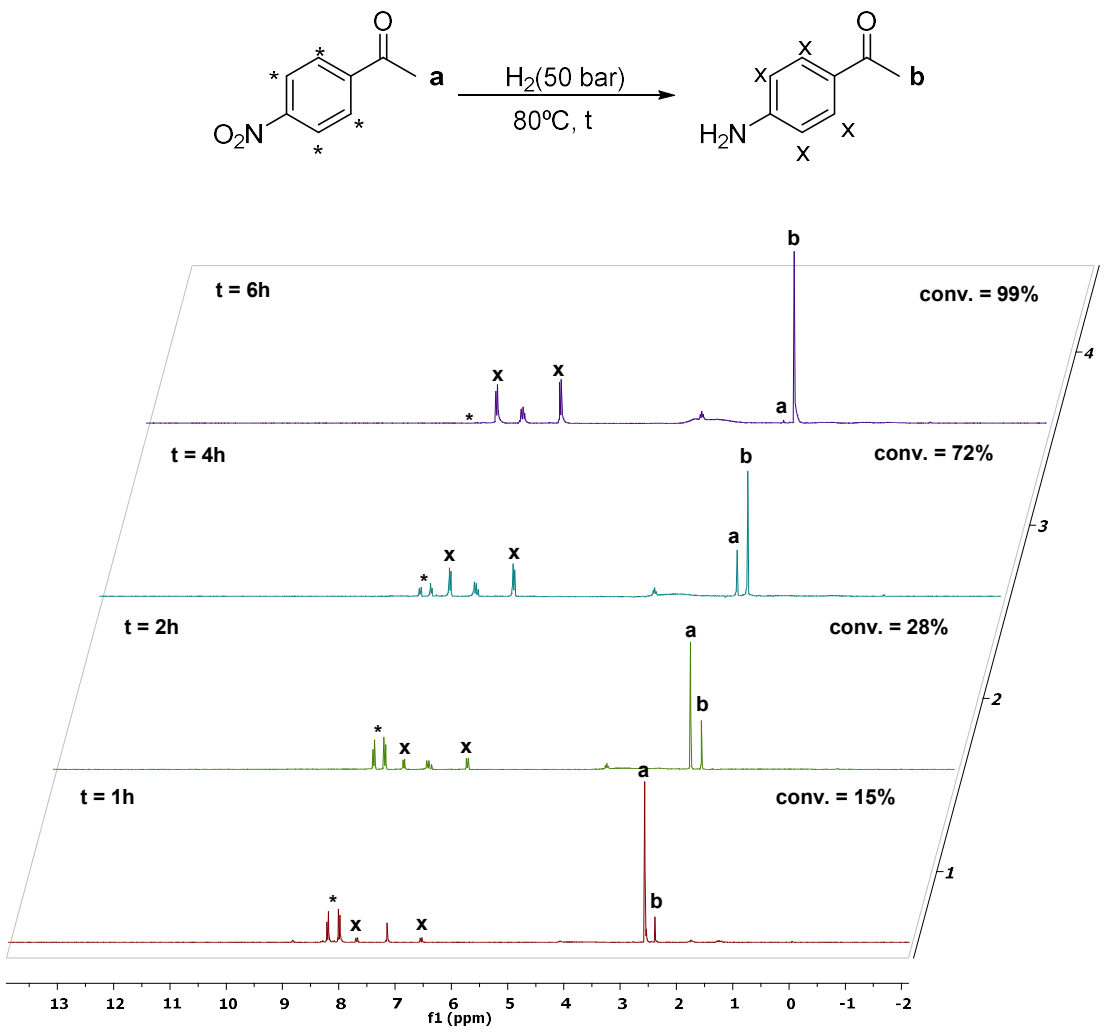

Figure S33. ^{1}H NMR monitoring of RhNPs-B catalyzed hydrogenation of *p*-benzoquinone (8)

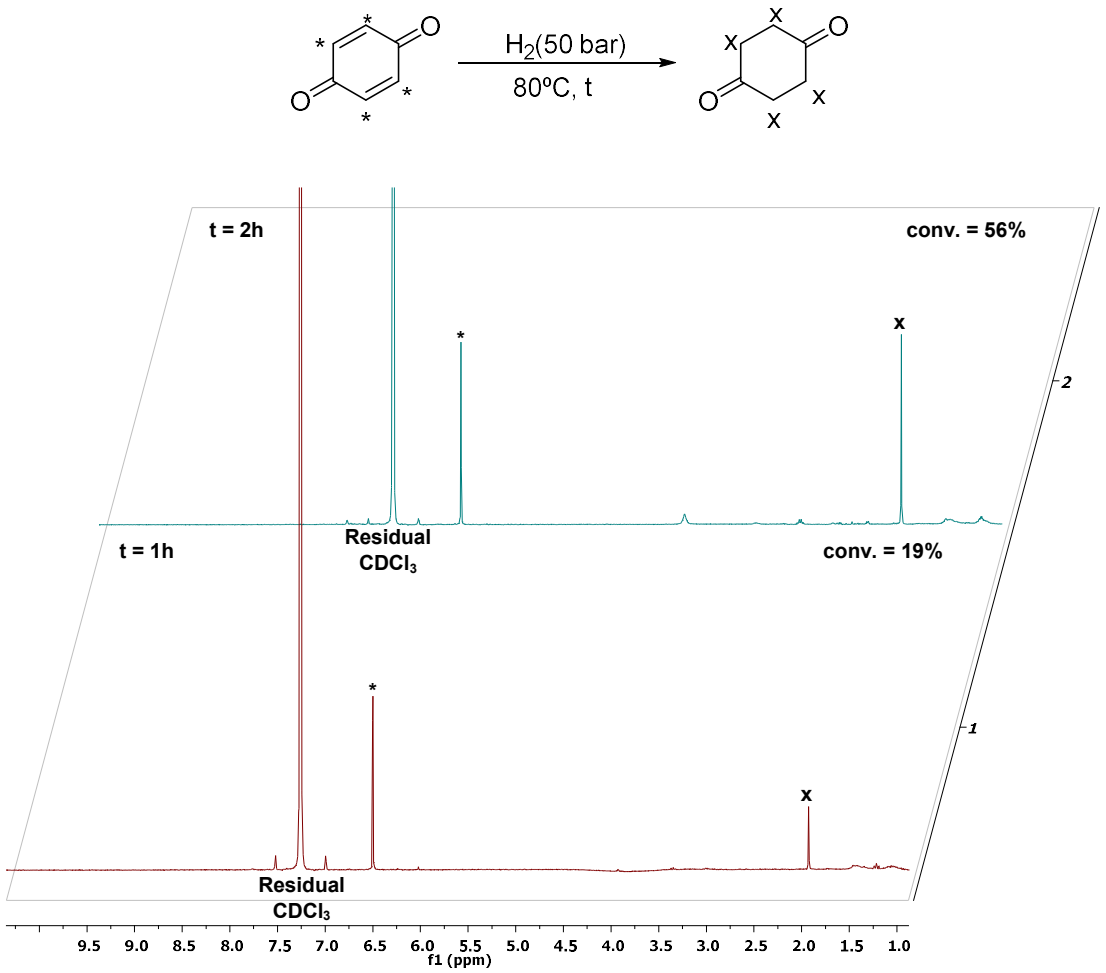

Figure S34. ^{1}H NMR spectrum of RhNPs-C-catalyzed hydrogenation of *p*-benzoquinone (8)

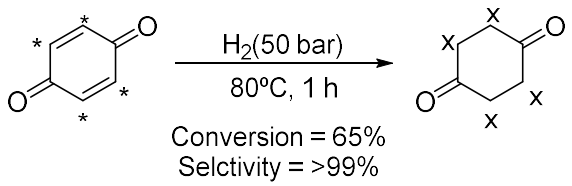

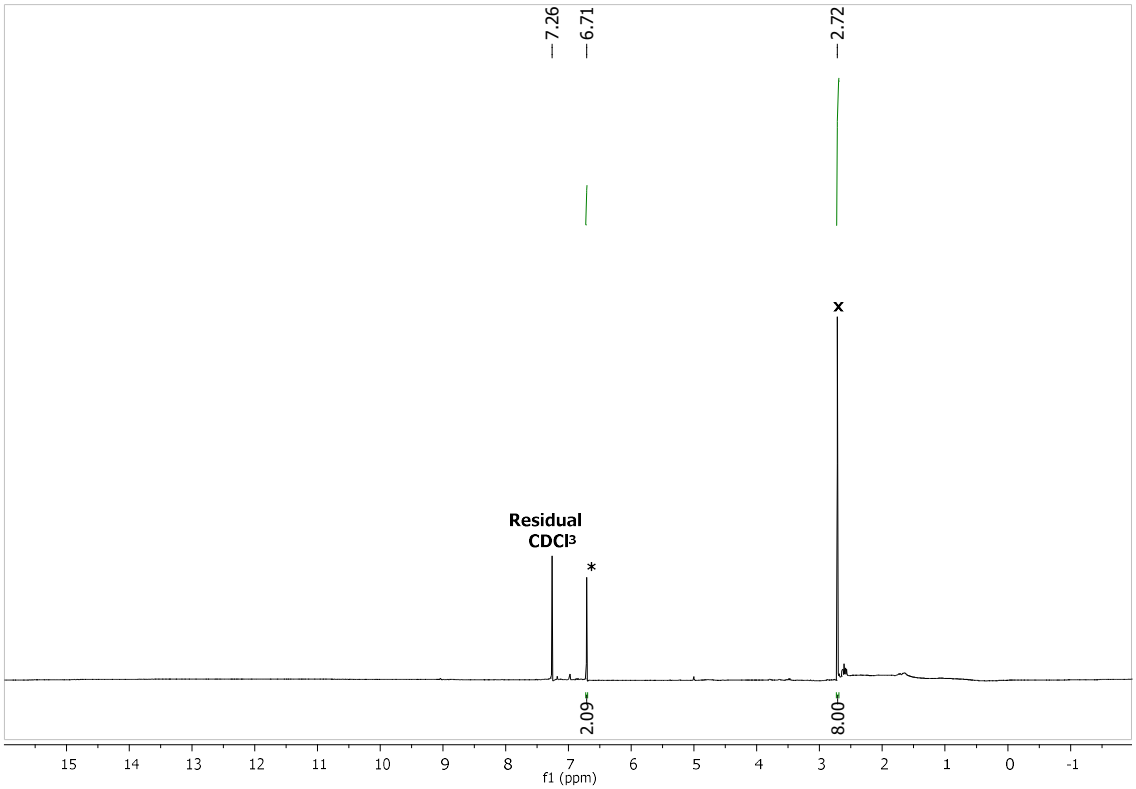

Figure S35. ^{1}H NMR of 4-aminoacetophenone. Hydrogenation product of 4-nitroacetophenone (5) catalyzed by RhNPs-C

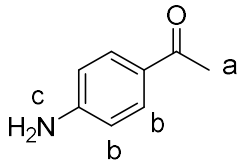

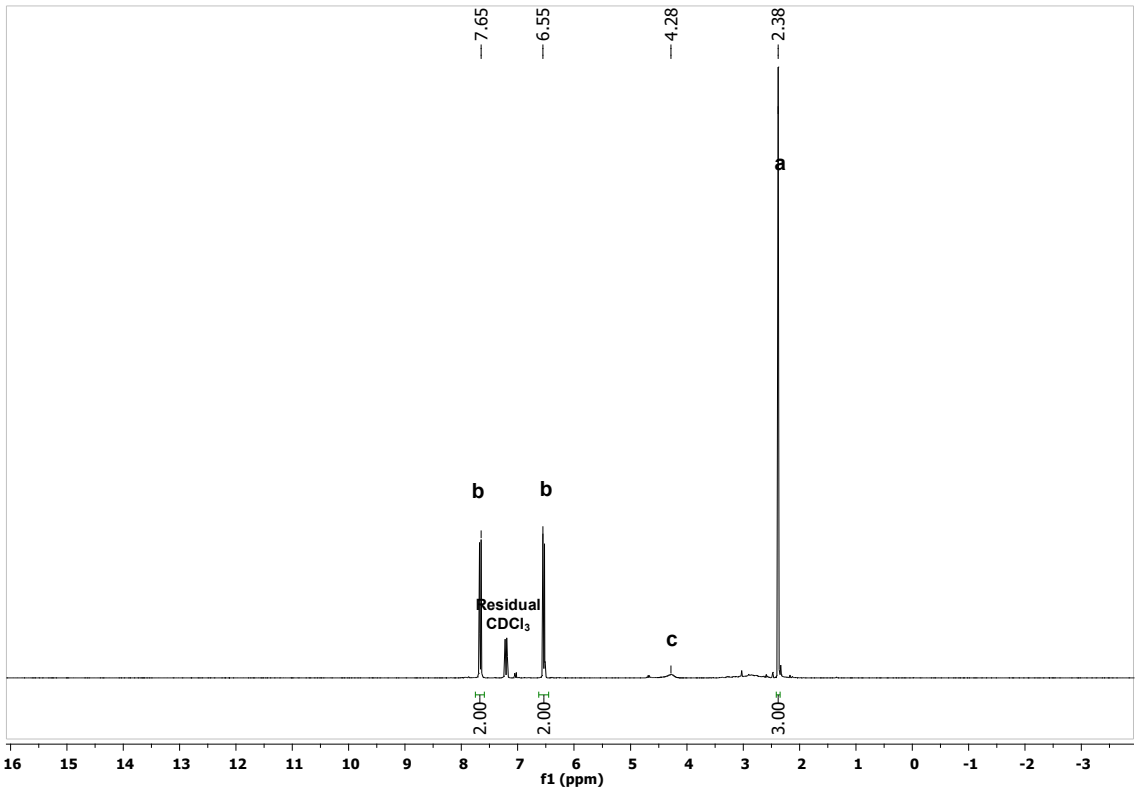

Figure S36. ^{1}H NMR of *N*-benzylaniline (product 10i)

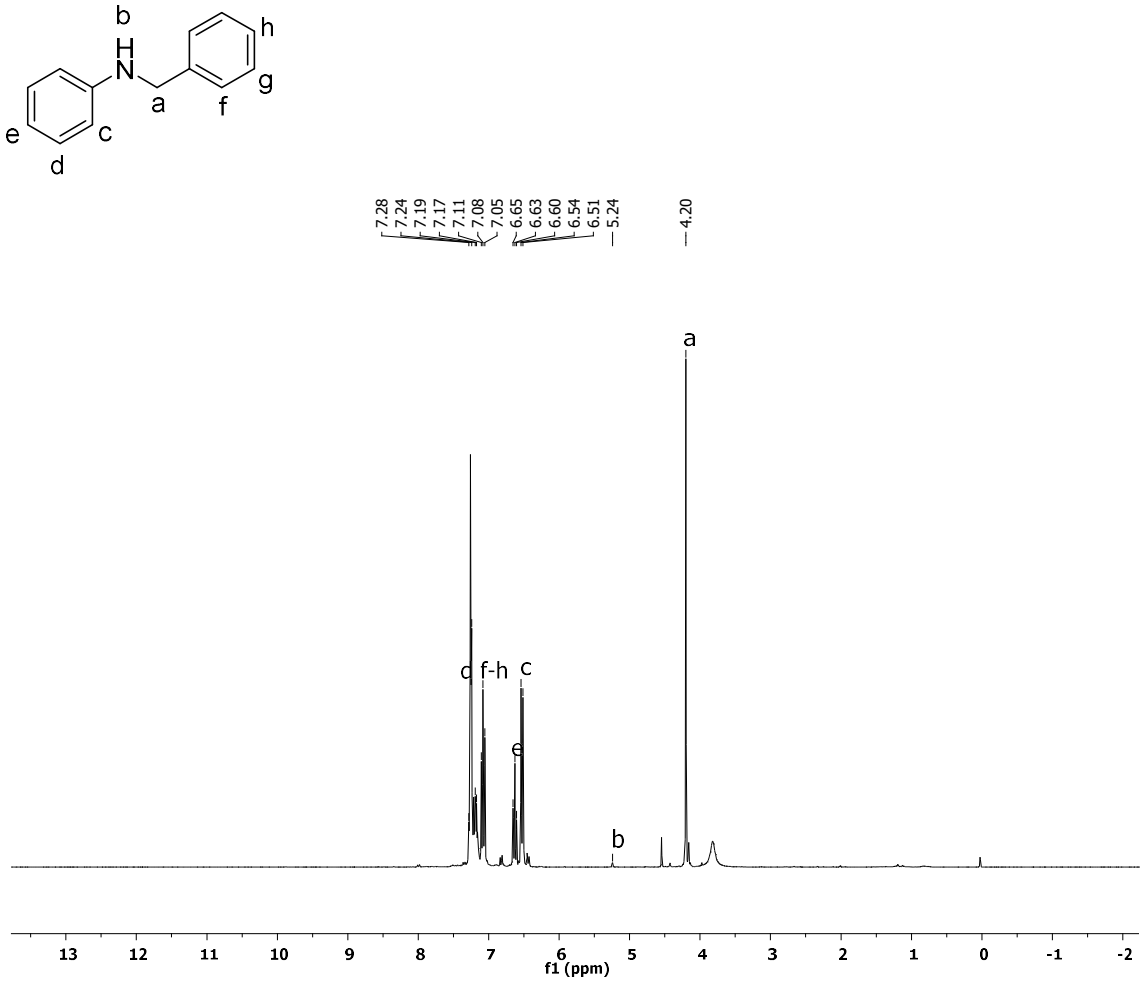

Table S6. Crystal data and structure refinement for $[Rh(\mu\text{-}SC_{12}H_{25})(COD)]_2$ (I)

Identification code	$[Rh(\mu\text{-}SC_{12}H_{25})(COD)]_2$	
Empirical formula	C40 H74 Rh2 S2	
Formula weight	824.93	
Temperature	100(2) K	
Wavelength	0.71073 Å	
Crystal system	Monoclinic	
Space group	P 21/m	
Unit cell dimensions	a = 8.734(3) Å	α= 90°.
	b = 26.987(8) Å	β= 90°.
	c = 8.390(2) Å	γ = 90°.
Volume	1977.6(10) Å3	
Z	2	
Density (calculated)	1.385 Mg/m3	
Absorption coefficient	0.966 mm-1	
F(000)	872	
Crystal size	0.100 x 0.050 x 0.010 mm3	
Theta range for data collection	2.264 to 26.842°.	
Index ranges	-11<=h<=11, -34<=k<=34, -10<=l<=10	
Reflections collected	55203	
Independent reflections	4314 [R(int) = 0.0881]	
Completeness to theta = 25.242°	99.9 %	
Absorption correction	Semi-empirical from equivalents	
Max. and min. transmission	0.7454 and 0.5740	
Refinement method	Full-matrix least-squares on F2	
Data / restraints / parameters	4314 / 1335 / 461	
Goodness-of-fit on F2	1.129	
Final R indices [I>2sigma(I)]	R1 = 0.0479, wR2 = 0.0972	
R indices (all data)	R1 = 0.0613, wR2 = 0.1026	
Extinction coefficient	n/a	
Largest diff. peak and hole	0.676 and -1.108 e.$Å^{-3}$	

Table S7. Crystal data and structure refinement of $[Rh(\mu\text{-}SC_6H_{11})(COD)]_2$ (II)

Identification code	$[Rh(\mu\text{-}SC_6H_{11})(COD)]_2$	
Empirical formula	C31 H53 Rh2 S2 · 0.5 C12 H14	
Formula weight	695.67	
Temperature	100(2) K	
Wavelength	0.71073 Å	
Crystal system	Monoclinic	
Space group	P 21/n	
Unit cell dimensions	a = 10.8550(4) Å	α= 90°.
	b = 28.6007(12) Å	β= 119.2390(10)°.
	c = 10.8441(4) Å	γ = 90°.
Volume	2937.7(2) Å3	
Z	4	
Density (calculated)	1.573 Mg/m3	
Absorption coefficient	1.284 mm-1	
F(000)	1444	
Crystal size	0.100 x 0.050 x 0.010 mm3	
Theta range for data collection	2.150 to 28.311°.	
Index ranges	-14<=h<=12, 38<=k<=0, 14<=l<=0	
Reflections collected	7462	
Independent reflections	7304 [R(int) = 0.0763]	
Completeness to theta = 25.000°	99.90%	
Absorption correction	None	
Max. and min. transmission	0.8621 and 0.5872	
Refinement method	Full-matrix least-squares on F2	
Data / restraints / parameters	7304 / 0 / 287	
Goodness-of-fit on F2	1.092	
Final R indices [I>2sigma(I)]	R1 = 0.0609, wR2 = 0.1195	
R indices (all data)	R1 = 0.0751, wR2 = 0.1255	
Extinction coefficient	n/a	
Largest diff. peak and hole	1.749 and -1.418 e.Å^{-3}	